View metadata, citation and similar papers at core.ac.uk

brought to you by CORE

provided by Missouri University of Science and Technology (Missouri S&T): Scholars' Mine

Scholars' Mine

Masters Theses

Student Theses and Dissertations

Fall 2010

Zinc iron phosphate glasses for enameling applications

Sagnik Saha

Follow this and additional works at: https://scholarsmine.mst.edu/masters_theses

 Part of the Materials Science and Engineering Commons

Department:

Recommended Citation

Saha, Sagnik, "Zinc iron phosphate glasses for enameling applications" (2010). *Masters Theses*. 4809.
https://scholarsmine.mst.edu/masters_theses/4809

This thesis is brought to you by Scholars' Mine, a service of the Missouri S&T Library and Learning Resources. This work is protected by U. S. Copyright Law. Unauthorized use including reproduction for redistribution requires the permission of the copyright holder. For more information, please contact scholarsmine@mst.edu.

ZINC IRON PHOSPHATE GLASSES

FOR ENAMELING APPLICATIONS

by

SAGNIK SAHA

A THESIS

Presented to the Faculty of the Graduate School of the

MISSOURI UNIVERSITY OF SCIENCE AND TECHNOLOGY

In Partial Fulfillment of the Requirements for the Degree

MASTER OF SCIENCE IN MATERIALS SCIENCE AND ENGINEERING

July 2010

Approved by

Dr. Richard K. Brow, Advisor

Dr. Delbert E. Day

Dr. F. Scott Miller

ABSTRACT

New compositions of low temperature black glasses were developed that are suitable as frits for enameling soda-lime silicate (S-L-S) glass substrates. Zinc iron phosphate glasses are of interest for this application because they possess dilatometric low softening points (under 600°C) and have coefficients of thermal expansion that are compatible with S-L-S glass (in the range 90-110x10^{-7}/°C). The development of compositions with excellent chemical durability, particularly in acidic conditions, is also desired. Compositional modification were made to the $(Na_2O+K_2O)\cdot ZnO\cdot MnO\cdot Fe_2O_3\cdot P_2O_5$ glass system using design of experiments. The compositional boundaries used in the design were based on earlier work at Missouri S&T. The Na_2O:K_2O molar ratio was fixed at 1:1 and the total alkali content was treated as a single compositional variable. Twenty glasses with compositions of ZnO (up to 20 mol%), MnO (up to 20 mol%), combined Na_2O and K_2O (up to 20 mol%), Fe_2O_3 (10-30 mol%) and P_2O_5 (40-60 mol%) were prepared and characterized. From this initial study, several additional compositions were prepared that had the desired properties for enameling soda-lime silicate glasses. These glass compositions were used for screen printing and firing onto soda lime silicate glasses. The screen printed films were fired at 680°C for 8 minutes.

Glasses of the system $(50-x)ZnO.xMnO.50P_2O_5$ were prepared with x=0, 10, 20, 30, 40 and glasses of the system $(50-x)ZnO.xMn_2O_3.50P_2O_5$ were made with x=0,10,20. The thermal properties and chemical durability were determined and UV-Vis spectroscopy was used to characterize these glasses.

ACKNOWLEDGMENTS

It has been a long and difficult journey for me to reach this point in my life. There have been a lot of people who have been part of this journey of mine without whom I would never have been successful. First, I would like to thank Dr. Richard Brow who has guided me throughout my Masters program and has accepted me the way I am. I would like to thank Dr. Steve Feller for being by my side from when I joined college until today. My heartiest gratitude also goes to Dr. Day and Dr. Miller for going through the thesis. I would also like to thank Dr. David Drain for walking me through the design of experiment processes and the entire glass research group (Mel, Lily, Nate, Zea, Xiaoming, Charmayne, Katie, Chris, Austin, Teng, Lina, Austin) for making this successful. My special gratitude goes to Dr. Mary Reidmeyer for helping me in screen printing and also for being nice to me. I would also like to thank Dr. Signo Reis for being helpful in my research. Thanks also to Dr. George Sakoske and Ferro Corporation for sponsoring this project.

It goes without saying that my family and friends have also had a major influence on me. First of all, I would like to thank my immediate family, Bimal Saha, Bratati Saha and Simba. I would also like to thank my extended family, Asok Motayed and Bhaskar Roy, for being a constant source of encouragement and help while I was pursuing my education. It would never have been possible if I did not have the support and companionship of my friends both from my undergraduate (Biswas, Ashish, Utsav, Dipak) and graduate (Arun, Gaurav, Argha, Bharat, Sumant, Abhinav, Sashwat) days.

TABLE OF CONTENTS

Page

LIST OF FIGURES

PART- 1 Page

PART- 2

LIST OF TABLES

PART -1 Page

PART-2

PART 1

ZINC IRON PHOSPHATE GLASSES FOR ENAMELING APPLICATIONS

1. INTRODUCTION

1.1 USE OF ENAMELS IN THE AUTOMOTIVE INDUSTRY

Black enamels on automotive windshields have been developed as a replacement for metal strips. Lead based sealing frits are commonly used for this application. However lead is toxic and hazardous for the environment. Research to develop lead-free enamels that are environmentally beneficial and those that would help auto manufacturers reduces costs and hazardous waste was desired.

1.2 DESIRED ENAMEL PROPERTIES

To develop enamels that can be applied to a soda lime glass windshield, various factors have to be taken into consideration. There is always a need in the market for better and cheaper alternative enamel compositions. The main criteria that need to be met are listed below-

1. The enamel needs to be applied to the soda lime glass at a temperature around 700 °C [1]. Since the enamel is sintered at the same time as the windshield is going to be shaped, the enamel should be thermally compatible with soda lime glass. For achieving this, the glass transition temperature of the enamel should be as low as possible. It would be preferable for the T_g to be less than 450°C [2].
2. The coefficient of thermal expansion of the enamel should match the coefficient of thermal expansion of the soda lime substrate glass. This will lead to minimum stress between the enamel and the substrate. During cooling the enamel may contract by a different amount than the substrate. If that happens shear stresses would be introduced at the interface. This could make the final product weak and

it could also lead to fracture of the enamel. The coefficient of thermal expansion for window glass is around 10.2×10^{-6}/ °C between 250 and 400°C. As a result, the target range for the CTE of the enamel was between $9.2\text{-}11.2\times10^{-6}$/ °C.

3. The enamel also must be chemically durable to withstand chemical degradation in harsh conditions. The dissolution rate of window glass is around 10^{-7}g/cm^2-min [3] in acidic conditions at around 80°C. Hence, it is desirable that dissolution rate of the enamel be comparable to the substrate glass. The target dissolution rate for automotive enamel at 80°C in acidic (pH~3) conditions is less than 10^{-7}g/cm^2-min.

1.3 ALKALI CONTAINED ZINC IRON PHOSPHATE GLASSES

Lead-based enamels have been used in the past because PbO has excellent fluxing and stabilizing abilities and provides good chemical durability [4]. To develop a composition that has high durability, low T_g, and the correct thermal expansion characteristics, without resorting to expensive, elaborate, or toxic modifiers, such as PbO, a different compositional family than the Pb-borosilicates should be used.

It is well known that typical phosphate glasses have poor chemical durability, though it varies with composition. The relatively poor chemical durability of phosphate glasses is generally attributed to the easily hydrated phosphate anions [5, 6]. Zinc iron phosphate glasses are of interest because of their potential to be excellent enamels; i.e., they possess low melting and softening temperatures and have a range of coefficients of thermal expansion [7]. T. Jermouni et al. have shown that glasses from the system $(0.5\text{-}x)ZnO\text{-}xFe_2O_3\text{-}0.5P_2O_5$ have low dilatometric softening temperatures, 460-480°C and

low dissolution rates near 10^{-7}g/cm^2.min, at 80°C in acidic conditions (pH=3), when the compositions are designed such that the O/P ratio falls in the range of 3.4-3.8 [8]. This was also shown in previous research at Missouri S&T (previously known as UMR) where zinc iron phosphate glasses with O/P ratio of 3.5 had the best durability [9]. In a previous research project it was also shown that glasses with ZnO (up to 20 mol%), Fe_2O_3 (10-20 mol%) and P_2O_5 (40-50 mol%) had the best combination of thermal and chemical properties [10]. Glasses modified with Na_2O and K_2O seemed to have the desired range of thermal properties and the addition of MnO proved to have a positive impact on the acid resistance of the enamel [11].

The purpose of the present study is to develop black glasses with a desired set of properties that would make them candidates for the necessary enameling applications. The compositional ranges for the $(Na_2O+K_2O) \cdot ZnO \cdot MnO \cdot Fe_2O_3 \cdot P_2O_5$ system compared to earlier studies have been expanded using a design of experiments approach to predict the compositional dependence of critical properties.

2. EXPERIMENTAL PROCEDURE

2.1 DESIGN OF EXPERIMENTS BY DEFINING THE EXPERIMENTAL REGION

Previous studies at Missouri S&T indicated that alkali containing zinc iron phosphate glasses have properties suitable for the desired enameling application [9,10]. The goal of the present work is to optimize the glass composition in the system $(Na_2O+K_2O)\cdot ZnO\cdot MnO\cdot Fe_2O_3\cdot P_2O_5$. A 'mixture design of experiments' was created using the Minitab statistical software package (Minitab @Release 14.1, 1972-2003 Minitab Inc.) utilizing a D-Optimal Design. This was determined by the constraints placed on the individual components in the mixture as well as any constraints involving more than one component [11]. Typically, each component would have an upper and lower bound. A D-optimal design is used when other classical designs do not apply or work. These designs are an option regardless of the model or resolution desired. D-optimal designs are straight optimizations based on chosen optimality criteria and the model that will be fit. The compositional boundaries used in the design are given in Table I. The constraints on the individual components used in the design, were in mole %. The Na_2O:K_2O molar ratio was fixed at 1:1 and the total alkali content was treated as a single compositional variable. The overall mixture constraint summed to 100%.

Table I: Compositional ranges used in the D-optimal design of experiments

Component	Range (mole%)
(Na_2O+K_2O)	0-20
ZnO	0-20
MnO	0-20
Fe_2O_3	10-30
P_2O_5	40-60

2.2 COMPOSITIONS CHOSEN TO BE TESTED EXPERIMENTALLY

Table II shows the glass compositions that were selected for the D-optimal design. The points chosen for the inclusion in this experimental design consisted of the extreme vertices (“corner points”), center of mass centroids (“interior points”) and the overall center of the experimental region [11]. The extreme vertices provide the most useful information because they spread the design out, and the interior points are helpful for detecting curvature in the response surface. Both the extreme vertices and interior points were thus included in the design, as well as the center point to estimate the experimental error variance.

Table II: Glass compositions from the D-optimal design (mole %)

ID	Na_2O+K_2O	ZnO	MnO	Fe_2O_3	P_2O_5	O/P	Annealing Temp(°C)
ZnFeP1	10	3.3	0	30	56.7	3.41	450
ZnFeP2	10	10	10	20	50	3.40	450
ZnFeP3	15	15	0	10	60	3.00	440
ZnFeP4	0	0	20	30	50	3.60	450
ZnFeP5	16.7	20	3.3	20	40	3.75	450
ZnFeP6	10	3.3	20	10	56.7	3.06	450
ZnFeP7	0	0	20	20	60	3.17	460
ZnFeP8	20	0	16.7	20	43.3	3.62	450
ZnFeP9	0	20	5	15	60	3.08	440
ZnFeP10	20	10	20	10	40	3.50	450
ZnFeP11	10	20	20	10	40	3.17	450
ZnFeP12	0	20	20	10	50	3.20	450
ZnFeP13	20	0	0	20	60	3.17	440
ZnFeP14	20	10	0	30	40	4.00	440
ZnFeP15	0	16.7	16.7	26.7	40	3.92	450
ZnFeP16	10	0	20	30	40	4.00	450
ZnFeP17	20	0	10	10	60	3.00	430
ZnFeP18	20	20	0	10	50	3.20	430
ZnFeP19	0	20	0	30	50	3.6	425
ZnFeP20	0	0	10	30	60	3.33	450

2.3 GLASS PREPARATION

Glasses were prepared using reagent grade raw materials, including Fe_2O_3, ZnO and $NH_4H_2PO_4$, mixed with K_2CO_3, Na_2CO_3 and MnO. The appendix provides information about the raw material sources. The batch size of all the glasses was 150 grams. The batch powders were ground in a mortar and pestle for five minutes to ensure good mixing, and then added to an aluminosilicate (fireclay) crucible. The crucible is manufactured by Canon Industrial Ceramics (DFC Ceramics- Product # C50021508). Batches were pre-reacted at 800°C for 30 minutes to remove ammonia. The crucible with the pre-reacted batch was then transferred to another furnace for melting in air for one hour at 1100°C. The crucibles were taken out of the furnace once after 30 minutes and the melts were stirred with a silica rod to help remove bubbles and to improve melt homogeneity. A portion of each melt was cast in molds ($2.5\times1\times0.5$ cm^3) for dilatometry experiments. The remainder of each melt was cast to form at least six corrosion samples ($1\times1\times1$ cm^3). Glasses were annealed for six hours at the temperatures given in Table II, based on glass transition temperatures determined by dilatometry.

2.4 THERMAL ANALYSIS OF GLASSES

Dilatometry was used to measure the glass transition temperature (T_g), the dilatometric softening point (T_d) and the coefficient of thermal expansion (CTE) for each sample. The samples for the dilatometer were approximately 25 mm in length. These bars were cut with an Isomet low-speed diamond saw and the ends were polished with 600 grit silicon carbide paper. Vernier calipers were used to determine whether the ends were parallel and to measure the sample lengths. An Orton Automatic Recording

Dilatometer (Model 1600) was used for these measurements. All measurements were done in air. The sample was heated at a rate of 10°C per minute to 600°C. The coefficient of thermal expansion (CTE) was calculated over the range of 250 – 400°C. This range was chosen to be below the glass transition temperature (T_g). The CTE was calculated using the slope of the percent linear change (PLC) vs. Temperature curve :

$$CTE = \frac{(PLC_{400} - PLC_{250})/100}{(400-250)^{\circ}C} \qquad (1)$$

The glass transition temperature was determined using the intersections of the two extensions of the length change vs. temperature results, above and below T_g. The dilatometric softening temperature (T_d) was taken as the temperature of maximum expansion for each sample, prior to softening.

2.5 CORROSION STUDIES

Annealed glass cubes ($1\times1\times1$ cm^3) were polished using 600 and 800 grit silicon carbide paper, and then carefully cleaned using acetone with fresh Kimwipes. The samples were then immersed in a dilute HCl solution with an initial pH ~ 3, contained in Nalgene bottles and maintained at 80°C. The samples were suspended using nylon thread. The glass surface area-to-solution volume ratio was fixed at 0.06 cm^{-1}. The initial weights of the samples were recorded, and the sample weights and the pH of the corresponding solution were recorded after 1 day, 2 days, 4 days, 1 week and 2 weeks on test. The samples were dried for 24 hours at room temperature before recording the weight loss and measuring the change of pH at the end of 1, 2, 4, 7 and 14 days. The dissolution rate (DR) was calculated using the relation:

$$DR = \frac{\Delta W}{SA \times t} \qquad (2)$$

where ΔW is the change in weight of the sample after time t, SA is the surface area of the sample, and t is the time in minutes.

2.6 SCREEN PRINTING

Screen printing is one method to apply a decorative or functional coating of the black enamels on a substrate. The optimized glass compositions were used for screen printing and firing onto soda lime silicate glasses. The soda lime glasses (Fisher Brand, Cat. No.:12-552) were cleaned using acetone and Kimwipes. Glass powders (< 45 microns) were obtained after crushing and sieving quenched glass. The glass was crushed with a steel crusher and hammer to a coarse grit and then ground in mortar and pestle. The powders were passed through a number 325 sieve to yield powder particle sizes under 45 microns.

Table III: Binder and Solvent combinations

Binder	Solvent
Elvacite 2046 2 wt% (iso-butyl methacrylate polymer)	50% volume of Butyl Carbitol Acetate [2-(2-Butoxyethoxy)Ethyl Acetate] and 50% volume of Butyl Cellulose 2-Butoxyethanol 99%

The pastes were created using the vehicle described in Table III. The solvent mixture (Manufacturer : Acros Organics) was poured in a glass container. A magnetic stir

bar was kept in the bottom of the container. The binder Elvacite 2046 was sprinkled to the solvent after a minute. The stirring continued for 2 hours.

The ratio of the weight of the powder to the weight of the solvent was kept between 4 and 6. A coarse mesh screen of 105M (131 microns) was chosen for this glass frit for the ink to easily move through the screen. The screen openings were at least three times the diameter of the powder particle.

The screens were printed using home-built equipment. The setup consisted of the screen frame held by a hinge system that allowed the screen to be indexed. The height of the screen above the substrate could also be set. The ink was forced through the screen with a plastic squeegee. Printing was done with the screen in full contact with the substrate. The screen printed samples were put in the dryer at 80°C overnight to evaporate the solvent. These films were then fired in air at 680°C for 8 minutes [1]. These are similar to processing conditions used to reshape windshields. One of the optimized glass compositions was also fired at 700 and 720°C for 8 minutes.

2.7 OPTICAL CHARACTERIZATION

Glass samples were polished to a 1200 grit finish on both sides, using SiC paper and water as lubricant. Sample thickness varied around 1-1.5 mm. The samples were then polished with 1μm Monocrystalline Diamond Suspension. Optical absorption spectra were collected with a Varian Cary 5 UV-VIS spectrophotometer operated in the 175-3300 nm range. All these optical spectroscopy experiments were performed at room temperature.

2.8 XRD CHARACTERIZATION

X-ray diffraction was performed using PANalytical X'Pert Materials research Diffractometer using Cu source (CuK-alpha radiation). Spectra were recorded using a step size of 0.03 and a step time of 2 seconds between angles of 6-70 º2θ.

3. RESULTS AND DISCUSSION

3.1 GLASS FORMATION

Most of the compositions tested exhibited good glass forming ability. The melts formed homogeneous glasses when cooled. This could be related to the high amount of P_2O_5 in the compositions. Every composition produced a shiny, black glass when quenched from the melt except for ZnFeP20. The ZnFeP20 melt crystallized to form a gray material upon quenching and this composition was not tested any further. Although the melts formed glasses after pouring, some of the unpoured material had crystallized inside the crucible. This could be related to slow cooling. Crystallization was determined by visual inspection.

3.2 THERMAL PROPERTIES

Up to three dilatometric samples were prepared and characterized for each composition and average values for T_g, T_d and CTE, with standard deviations, are summarized in Table IV. The glass transition temperature for these glasses ranged from 408°C to 460°C, the softening temperature ranged between 452°C to 508°C while the CTE ranged between $7.1\times10^{-6}/\,^\circ$ C to $15.1\times10^{-6}/\,^\circ$ C**.** Figure 1.1 shows how CTE for these glasses increases with the increase of the alkali content.

Table IV: Summary of thermal properties from dilatometric measurements

ID	Tg(° C)	Td (° C)	CTE($\times 10^{-6}$/ ° C)
ZnFeP1	434±8	496±12	12.8±0.5
ZnFeP2	449±5	496±4	9.4±2.8
ZnFeP3	411±11	459±10	12.7±0.4
ZnFeP4	458±6	503±6	8.4±1.9
ZnFeP5	411±8	452±2	14.7±0.6
ZnFeP6	457±4	508±4	11.2±1.0
ZnFeP7	455±13	505±10	10.0±1.0
ZnFeP8	445±10	485±9	16.0±0.1
ZnFeP9	446±9	502±8	8.1±1.7
ZnFeP10	442±5	479±2	15.1±0.4
ZnFeP11	458±7	493±1	12±1.1
ZnFeP12	436±6	485±8	7.1±1.3
ZnFeP13	432±1	483±7	14.3±0.4
ZnFeP14	456±5	497±3	14.9±0.1
ZnFeP15	443±11	484±10	10.3±0.2
ZnFeP16	460±8	498±2	13.0±1.1
ZnFeP17	452±6	500±5	14.2±0.4
ZnFeP18	432±6	471±6	14.9±0.2
ZnFeP19	408±1	464±4	7.8±1.3

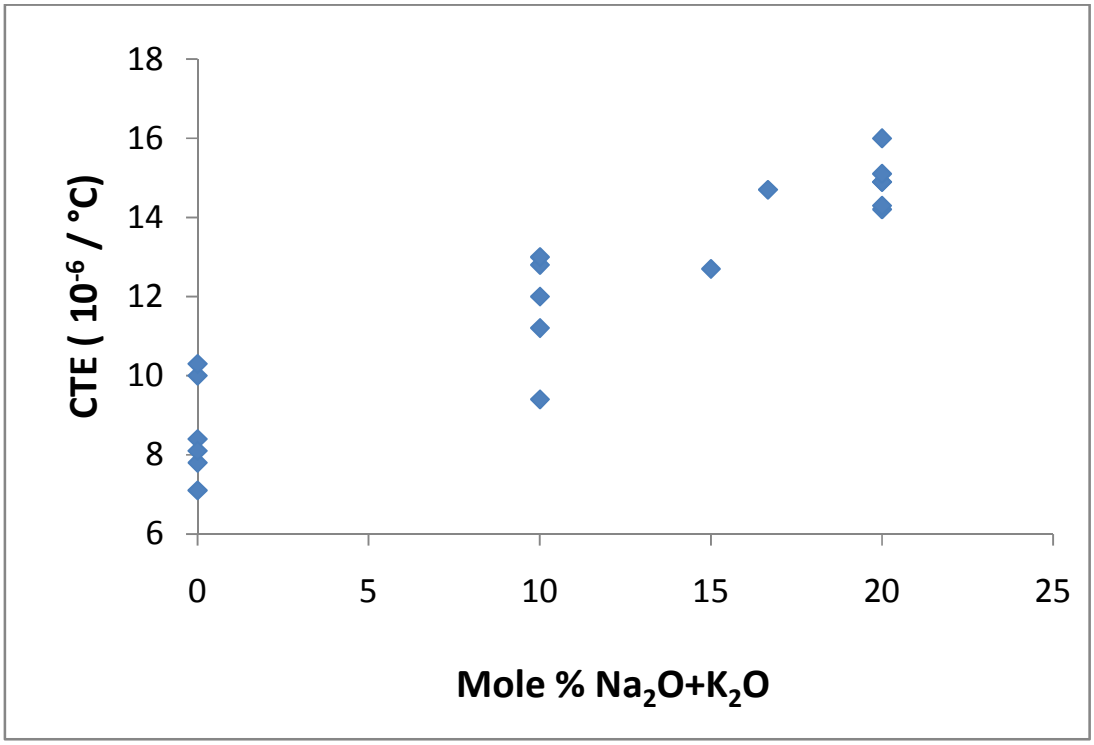

Figure 1.1: Relationship between CTE and Na_2O+K_2O content

3.3 CHEMICAL DURABILITY RESULTS

For the corrosion experiments three replicates for each composition were tested and the average dissolution rate with the standard deviation is reported. Figure 1.2 shows the weight losses for different glasses at 80°C. In general the weight loss rate decreases after longer times (>4-7 days) in dilute HCl.

Table V summarizes the total weight losses after different times at 80°C, and the pH of the solution at the conclusion of each experiment. Several samples fragmented over the course of these experiments and those samples are indicated with an 'X' in Table V. Several glasses like ZnFeP14 and ZnFeP17 showed increase of weight with time. This could be related to films which were visible that formed on the surface of the glasses.

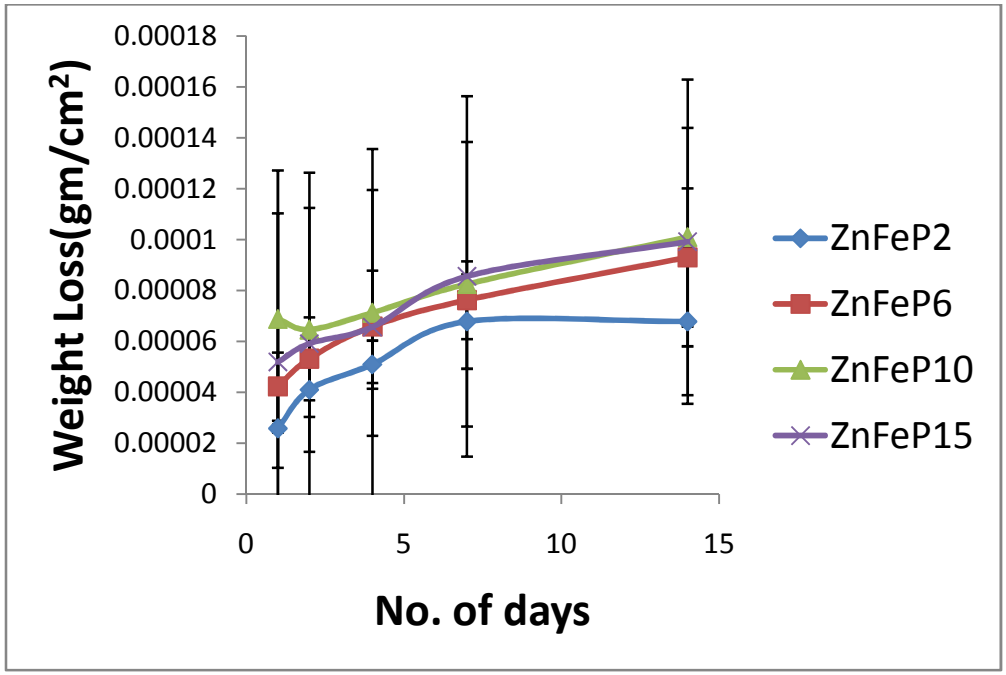

Figure 1.2: Cumulative weight loss for selected glass at 80°C HCl(initial pH=2.95)

Table V: Dissolution rates for glasses in HCl (initial pH ~ 3) at 80°C

ID	Dissolution rate ($g/cm^2.min$)	Log (DR) $Log(g/cm^2.min)$	Sol'n pH at 14 days
ZnFeP1	2.66×10^{-7}(After 4 days)	-6.6	X
ZnFeP2	4.69×10^{-9}	-8.5±0.1	2.74±0.15
ZnFeP3	6.67×10^{-8}	-7.2	2.92
ZnFeP4	2.54×10^{-8}(After 7 days)	-7.6	2.87
ZnFeP5	6.02×10^{-9}	-7.7±0.3	3.00±0.06
ZnFeP6	4.61×10^{-9}	-8.3±0.1	3.23±0.24
ZnFeP7	2.63×10^{-7}	-6.6	X
ZnFeP8	2.91×10^{-9}	-8.5±0.2	3.06±0.04
ZnFeP9	X(Cracked by first day)	X	X
ZnFeP10	5.0×10^{-9}	-8.3±0.2	2.99±0.06
ZnFeP11	2.89×10^{-9}	-8.5±0.3	4.29±2.25
ZnFeP12	4.4×10^{-9}	-8.4±0.1	3.13±0.25
ZnFeP13	2.9×10^{-7}	-6.6	2.83
ZnFeP14	3.46×10^{-9}	-8.5±0.4	3.11±0.21
ZnFeP15	4.92×10^{-9}	-8.3±0.3	2.98±0.03
ZnFeP16	4.22×10^{-9}	-8.4±0.7	3.22±0.22
ZnFeP17	2.24×10^{-8}	-7.7±0.1	3.24±0.18
ZnFeP18	4.34×10^{-8}	-7.4±1.2	3.65±0.01
ZnFeP19	3.92×10^{-8}(After 1 day)	-7.4	X

3.4 FITTING THE EMPIRICAL MODELS WITH MINITAB

MINITAB was used to analyze the compositional dependences of the thermal properties of the glasses. The simplest model is a linear model that ignores cross-correlations between components. The following property-composition equations were developed from the linear models:

$$T_g\ (°C) = 4.44[Na_2O+K_2O] + 3.73[ZnO] + 5.41[MnO] + 4.46[Fe_2O_3] + 4.32[P_2O_5] \quad (3)$$

$$T_d\ (°C) = 4.33[Na_2O+K_2O] + 3.89[ZnO] + 5.36[MnO] + 4.81[Fe_2O_3] + 5.10[P_2O_5] \quad (4)$$

$$CTE\ (\times 10^{-6}/°C) = 0.42[Na_2O+K_2O] + 0.08[ZnO] + 0.11[MnO] + 0.13[Fe_2O_3] + 0.06[P_2O_5] \quad (5)$$

Based on the component parameters, the property composition equations indicate, for example, that increasing ZnO contents reduce the characteristic temperatures, and increasing the alkali contents increase CTE (Figure 1.1). Figure 1.3 shows the correlation between the predicted (equation 4) and measured (Table II) values of T_d and Figure 1.4 shows the predicted (equation 5) and measured (Table II) values of CTE. These figures indicate the relative precision of the Minitab predictions. There is greater scatter in the T_d data and this is reflected in the associated regression squares for the responses, calculated by Minitab to be 52.6% for T_d and 89.8% for CTE.

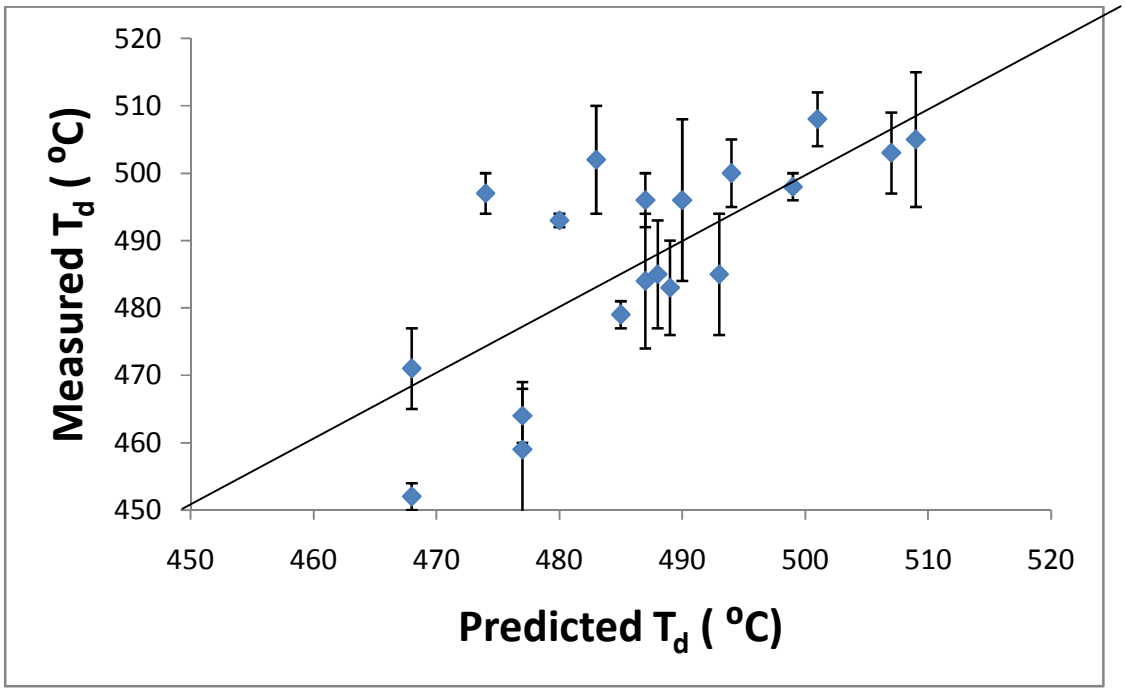

Figure 1.3: Relationship between measured T_d and predicted T_d

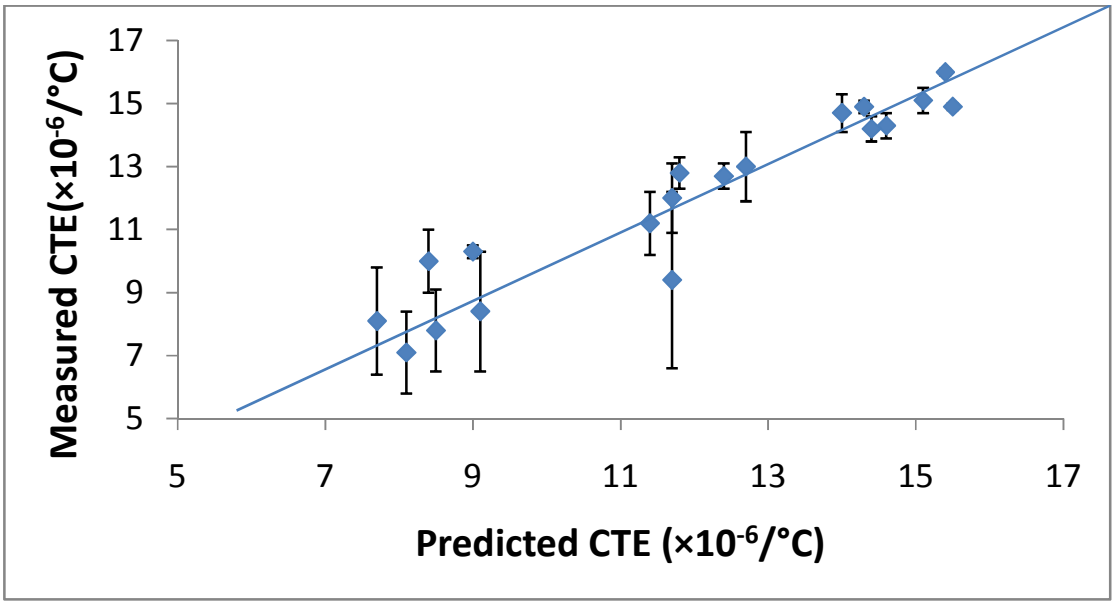

Figure 1.4: Relationship between measured CTE and predicted CTE

Figures 1.5 and 1.6 show examples of contour plots for the compositional dependences of CTE. These figures clearly show that increasing the alkali (Na_2O+K_2O) content increases CTE. Figures 1.7 and 1.8 show examples of contour plots of the compositional dependence of T_d. It is apparent that increasing ZnO reduces T_d. These mixture contour plots give the compositional trends of the respective properties. The small triangle in the mixture contour plot is the actual compositional range that was used to model this design. The numbers on the corners are the highest possible mole % of the given component while the numbers on the axis are the lowest possible mole % of the components, if the model is extended beyond the compositional boundaries used.

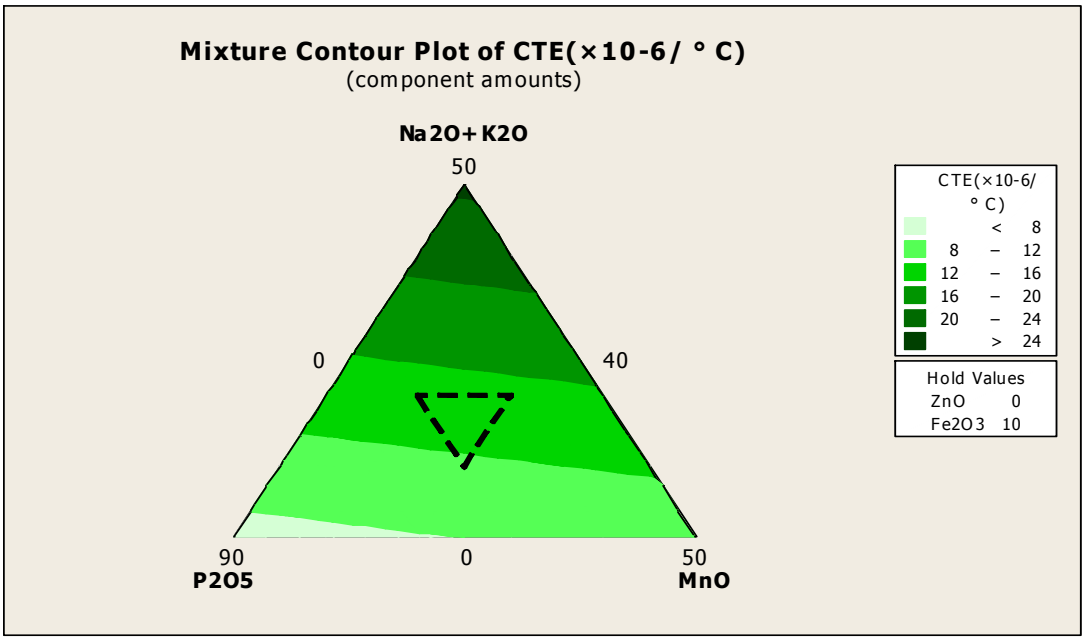

Figure 1.5: Mixture contour plot for CTE with ZnO fixed at 0 mole % and Fe_2O_3 fixed at 10 mole %

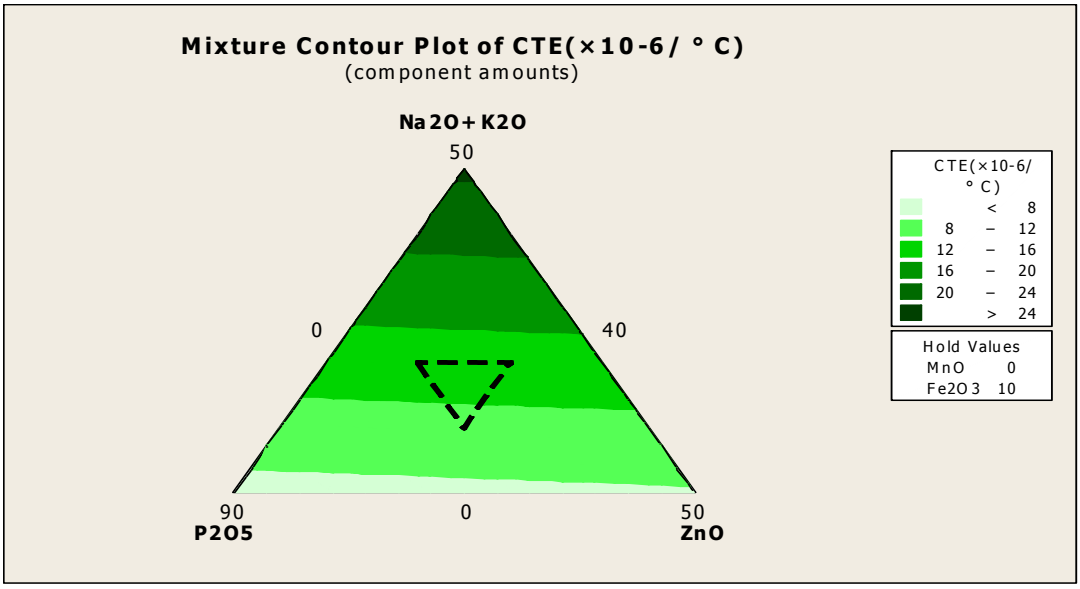

Figure 1.6: Mixture contour plot for CTE with MnO fixed at 0 mole % and Fe_2O_3 fixed at 10 mole %

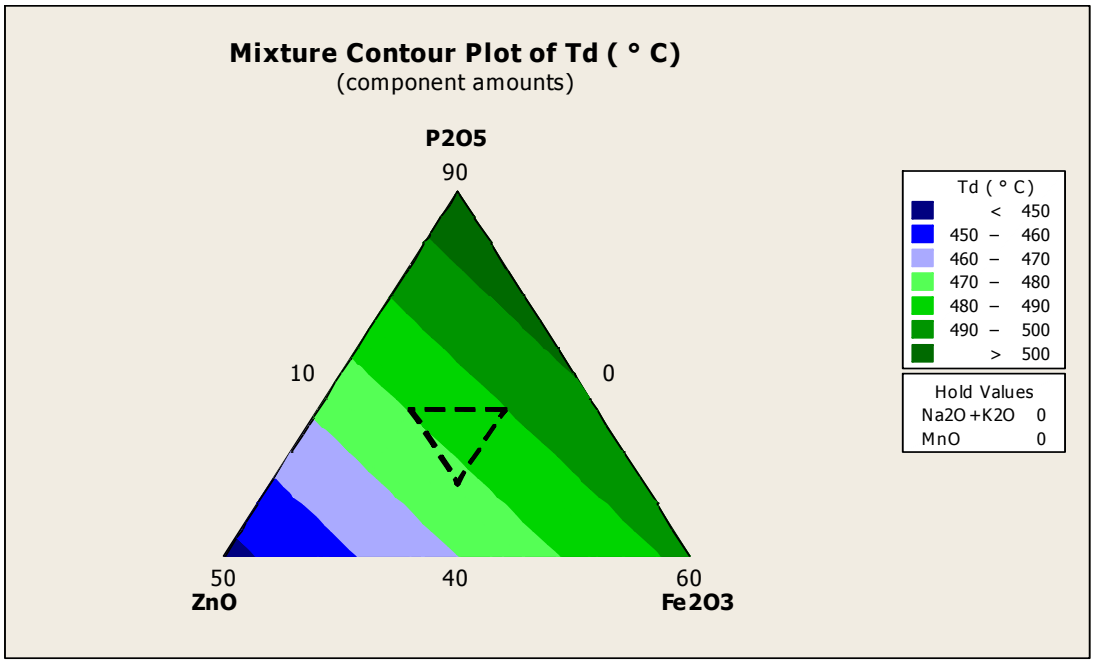

Figure 1.7: Mixture contour plot for T_d with (Na_2O+K_2O) fixed at 0 mole % and MnO fixed at 0 mole %

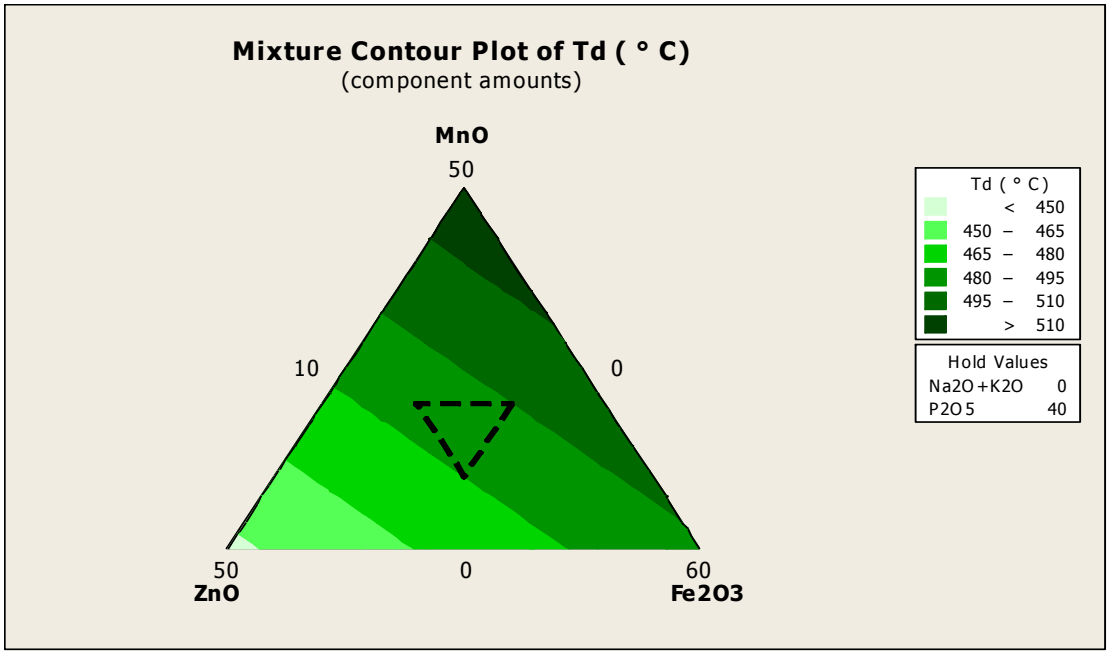

Figure 1.8: Mixture contour plot for T_d with (Na_2O+K_2O) fixed at 0 mole% and P_2O_5 fixed at 40 mole %

Minitab was again used to analyze the compositional dependence of the log of dissolution rate, using the 14 day weight loss values and the following linear model was developed:

$$\log(DR) = -0.08[Na_2O+K_2O] - 0.09[ZnO] - 0.13[MnO] -0.09[Fe_2O_3] -0.06[P_2O_5] \quad (6)$$

where DR is given in g/cm^2-min. Figure 1.9 shows the relationship between the predicted and experimental dissolution rates. The regression square for this response was 57.4%.

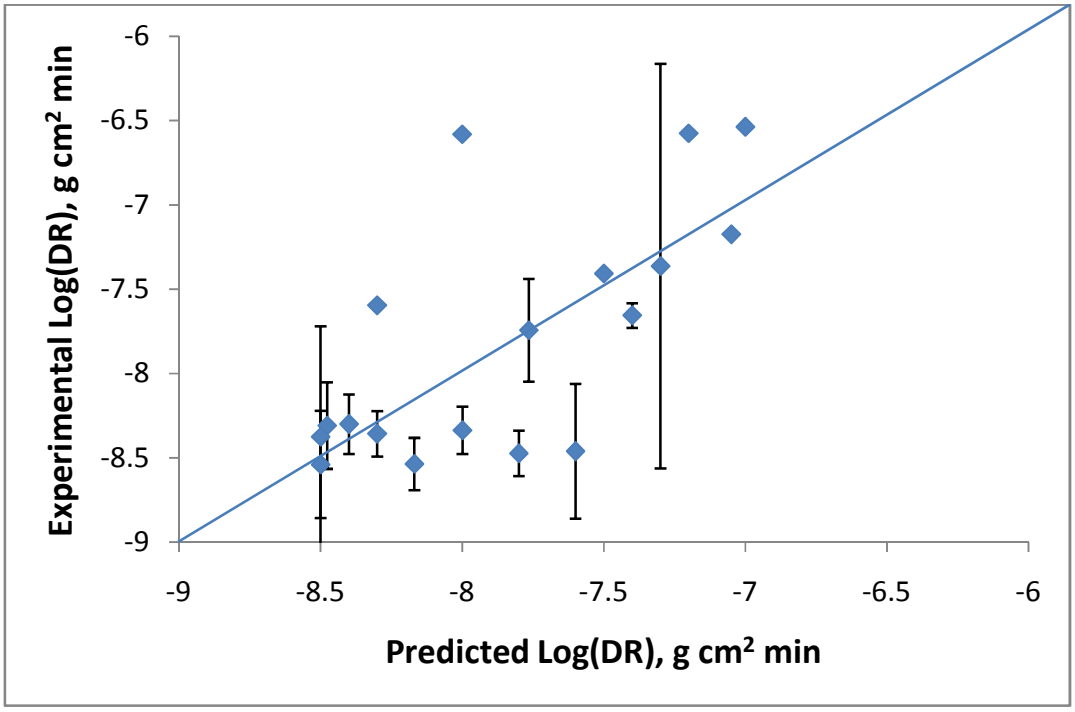

Figure 1.9: Relationship between measured log(DR) and predicted log(DR)

Equation 4 indicates that increasing the MnO and Fe_2O_3 contents of the glass have the greatest effects on reducing the weight loss rates in dilute HCl for 14 days. Similar conclusions can be drawn from the contour plots shown in Figures 1.10 and 1.11.

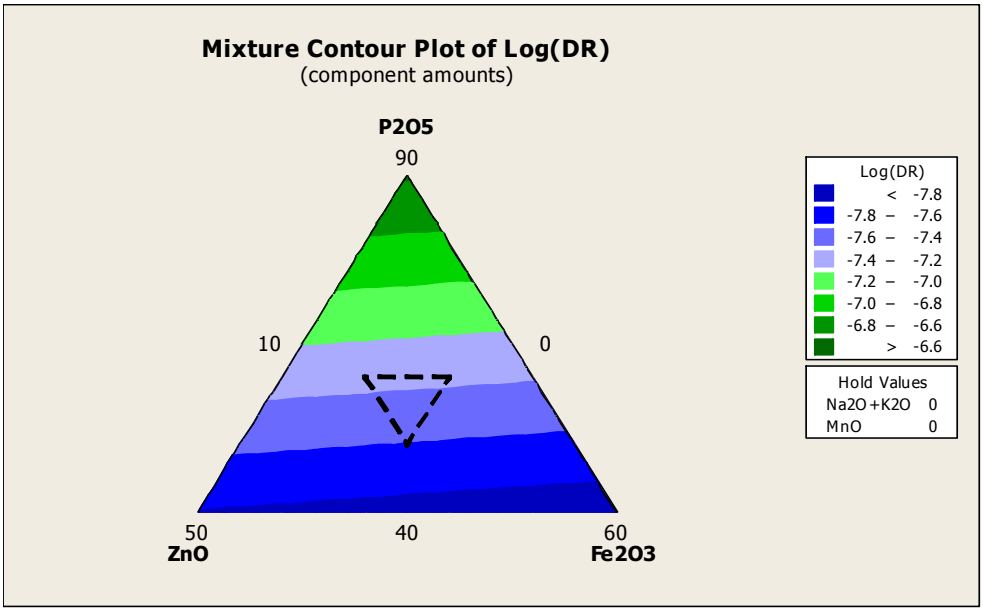

Figure 1.10: Mixture contour plot for log(DR) with (Na_2O+K_2O) and MnO both fixed at 0%

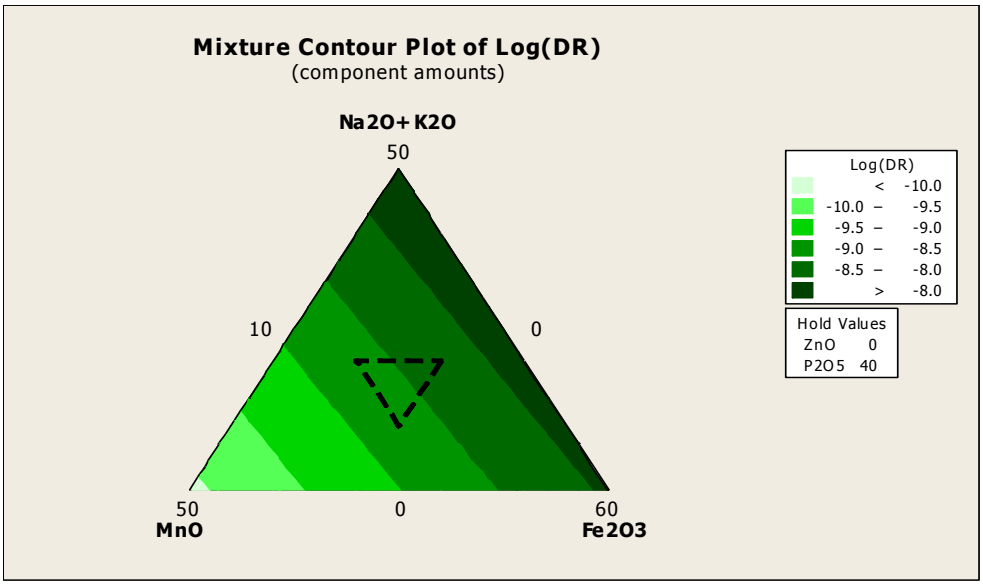

Figure 1.11: Mixture contour plot for log(DR) with ZnO fixed at 0 mole% and P_2O_5 fixed at 40 mole%

3.5 OPTIMIZE GLASS COMPOSITION FOR MODEL VERIFICATION

A second statistical tool called the Design Expert was used with the data from the initial 19 glass compositions to determine optimum compositions with the desired properties, including the lowest possible softening temperature, the lowest possible corrosion rate and a CTE in the range of 9.2-11.2×10^{-7}/°C. The predicted optimized glass compositions are listed in Table VI. The optimized glass compositions were melted using the same technique used to melt the initial 20 glasses.

Table VI: Optimized Glass compositions (mole %) including the predicted properties

Na_2O+K_2O	ZnO	MnO	Fe_2O_3	P_2O_5	T_g (°C)	T_d (°C)	CTE (10^{-6}/°C)	Log(DR) [Log(g/cm^2.min)]	Desirability
0	10	20	30	40	446	486	10.3	-8.9	0.841
0	0	18.7	30	51.3	450	497	9.9	-8.6	0.755
5	20	20	10	45	437	474	11	-8.5	0.727
0	20	10	30	40	432	474	9.9	-8.4	0.693

Desirability is an objective function that ranges from zero outside of the limits (least desirable) to one at the goal (most desirable). The numerical optimization finds a point that maximizes the desirability function. The characteristics of a goal may be altered by adjusting the weight or importance. Desirability is simply a mathematical method to find the optimum.

Figure 1.12 shows the XRD pattern for a powder of the quenched ZnFeP21 composition. There is no evidence for crystallization in this sample.

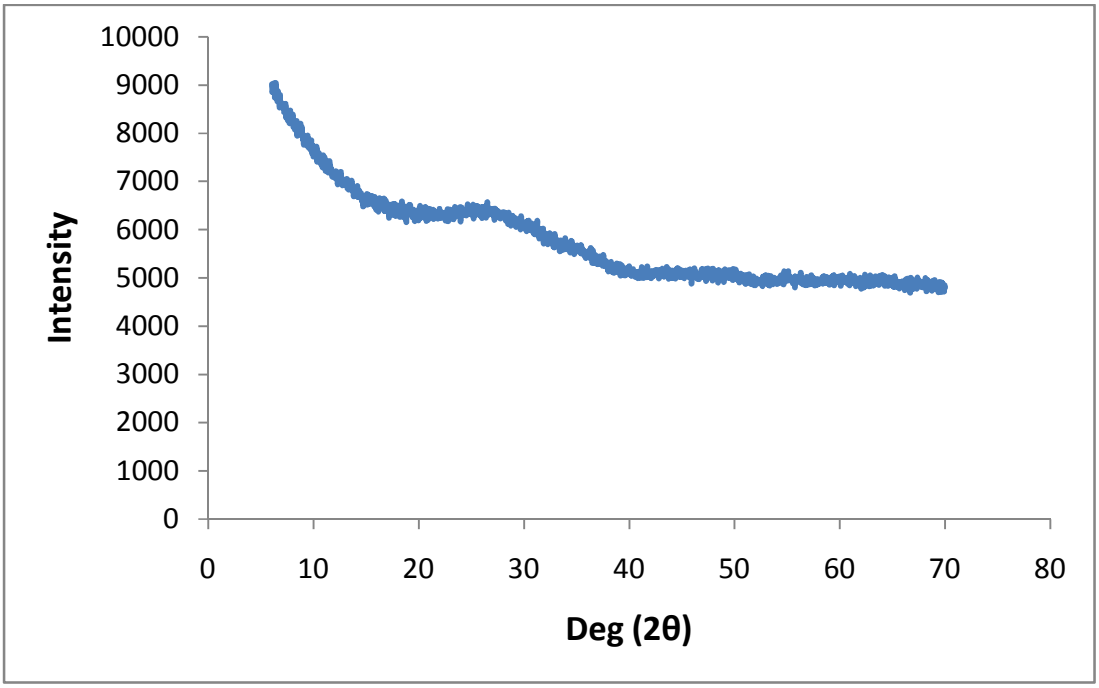

Figure 1.12: XRD pattern for ZnFeP21

3.6 PROPERTIES OF OPTIMIZED GLASSES

The thermal properties of the optimized glasses were measured using dilatometry as were the thermal properties of the soda lime silicate glass. These properties are listed in Table VII, and the dilatometric curves are shown in Figure 1.13. The measured characteristic temperatures are higher than the predicted temperatures and the measured CTEs are lower than predicted CTEs.

Table VII: Summary of thermal properties of the optimized glasses and a soda lime glass

ID	Exp. T_g(°C)	Predicted T_g(°C)	Exp. T_d(°C)	Predicted T_d(°C)	Exp. CTE($\times 10^{-6}$/ °C)	Predicted CTE($\times 10^{-6}$/ °C)
ZnFeP21	461±11	446	507±4	486	10.0±0.8	10.3
ZnFeP22	504±6	450	555±2	497	8.4±0.9	9.9
ZnFeP23	484±5	437	526±3	474	9.3±0.5	11
ZnFeP25	481±6	432	525±2	474	8.3±0.8	9.9
SLS	514±10		583±11		10.2±0.3	

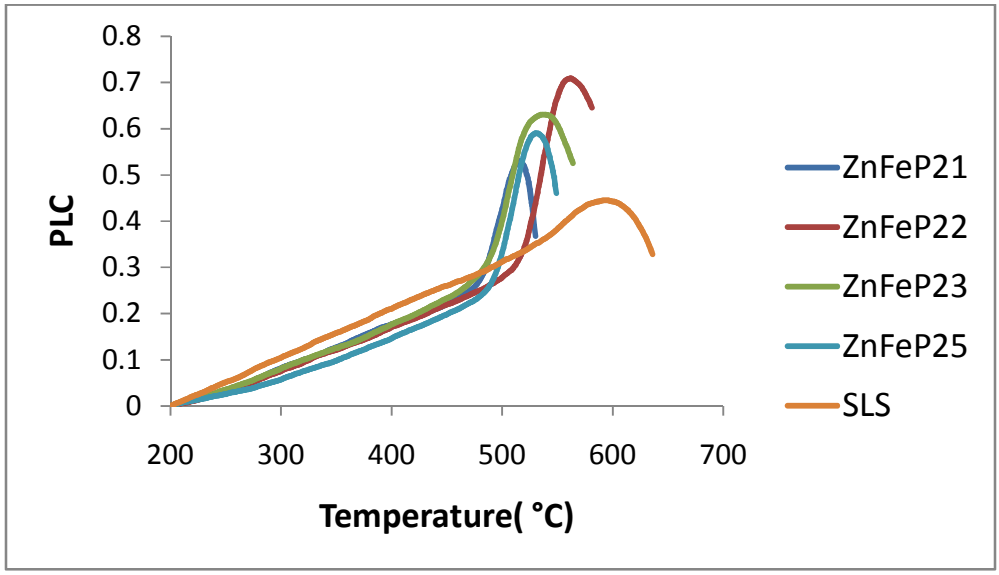

Figure 1.13: Dilatometric curves of SLS and the optimized glasses

Corrosion tests were carried out for these optimized glasses to determine the durability in 80°C in a HCl solution with initial pH of 3.4. Figure 1.14 and Table VIII summarize the total weight losses of the four optimized compositions after different times for two weeks. Glass ZnFeP22 was also tested but those samples cracked during the dissolution experiments and so an accurate dissolution rate was not determined.

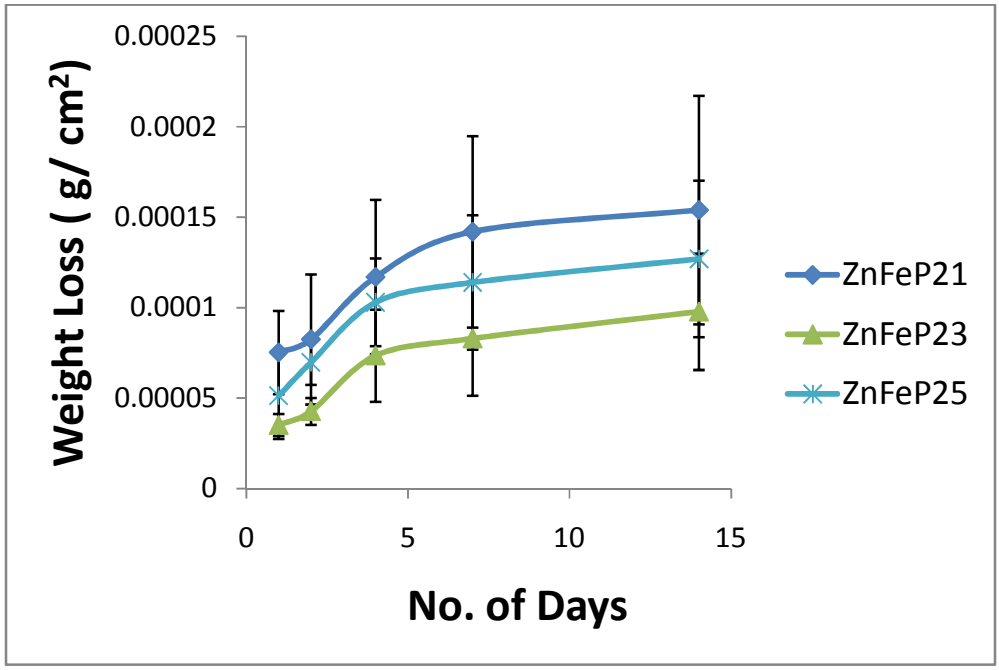

Figure 1.14:Weight loss from optimized glasses at 80°C HCl(initial pH=3.4)

Table VIII: Summary of dissolution rates for optimized glasses in HCl (pH = 3.4) at 80°C

ID	Dissolution rate ($g/cm^2.min$)	Sol'n pH at 14 days	Predicted log(DR)	Experimental log(DR)
ZnFeP21	7.62×10^{-9} $\pm3.14\times10^{-9}$	2.94±0.16	-8.9	-8.1±0.2
ZnFeP22	Samples cracked when immersed in water	X	-8.6	-8.8(After 7 days)
ZnFeP23	4.85×10^{-9} $\pm1.59\times10^{-9}$	3.16±0.04	-8.5	-8.7±0.6
ZnFeP24	6.28×10^{-9} $\pm2.14\times10^{-9}$	2.98±0.11	-8.4	-8.2±0.2

3.7 OPTICAL CHARACTERIZATION OF OPTIMIZED GLASSES

Figure 1.15 shows the different colors of the optimized glasses. All these glasses were black in color. These black glasses were between 1 to 1.25 mm thick. Figure 1.16 shows the UV-VIS spectra collected from the optimized glasses. These glasses do not transmit in the visible spectrum or the near IR (~1200 mm), which is consistent with their black color as shown in Figure 1.15.

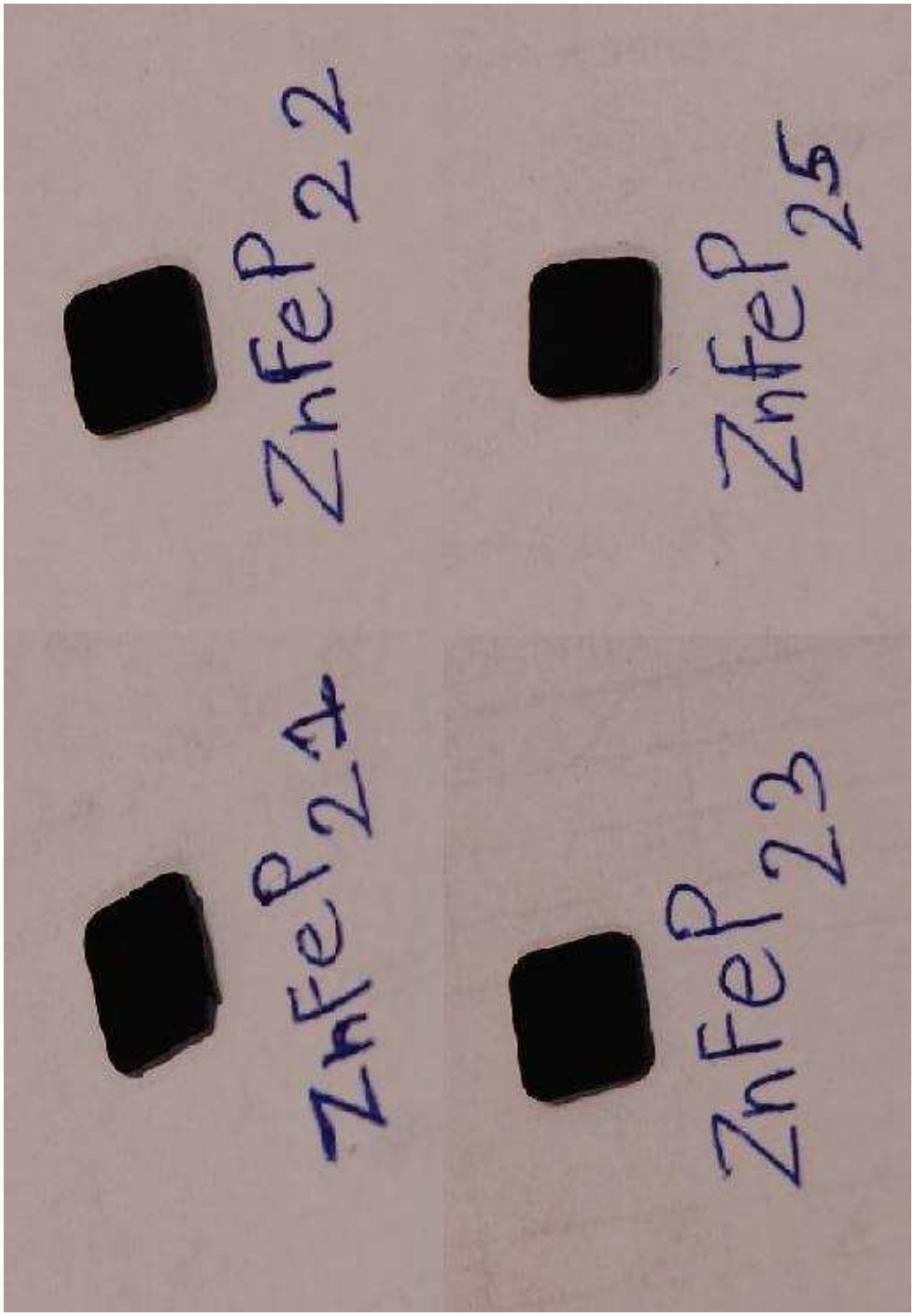

Figure 1.15: Showing the colors obtained from the optimized glasses

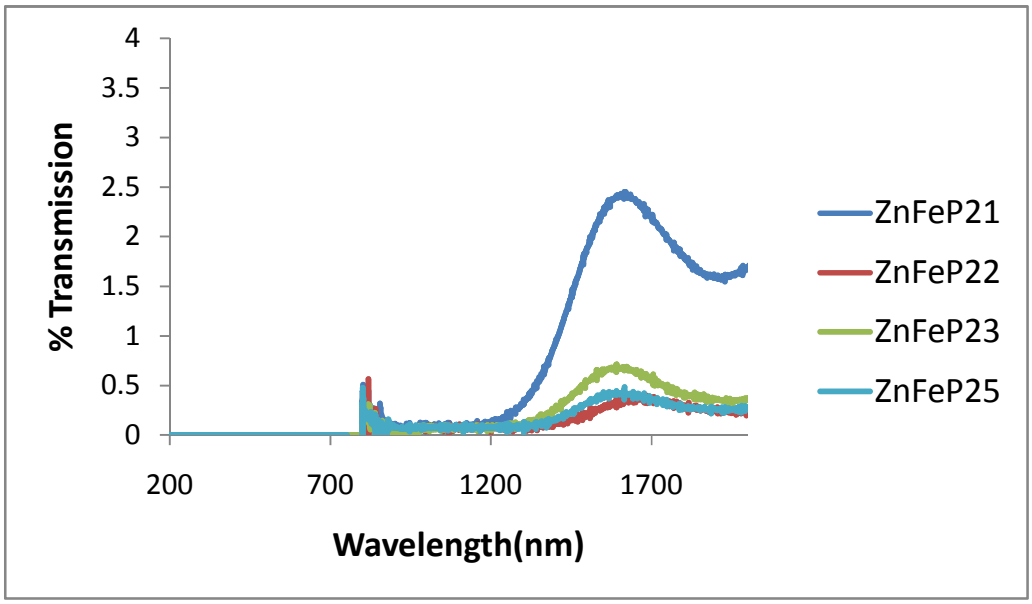

Figure 1.16: UV-VIS spectra of the optimized glasses

3.8 SCREEN PRINTING OF OPTIMIZED GLASSES

The thickness of the screen printed samples was measured with vernier calipers before and after they were fired at 680°C for 8 minutes. The initial thickness of soda lime silicate glasses and the final thickness of the deposited films on the soda lime silicate glasses were measured to get the thickness of the deposited films. The printed films were about 100 microns thick and the fired films were about 50-80 microns thick. The coatings of ZnFeP21 and ZnFeP22 were dark grey in color whereas the color of ZnFeP23 was light grey. This is because the ZnFeP23 had a lower content of Fe_2O_3 in comparison to the other optimized glasses. The compositions ZnFeP21 and ZnFeP22 seemed to wet and bond to the substrate well at 680°C. The compositions ZnFeP23 and ZnFeP25 had very little adherence to the substrate. These films flaked off when scratched with a fingernail. Samples of the ZnFeP21 composition were fired at 700°C and at 720°C for 8 minutes.

Figure 1.17 shows optical micrographs of the surfaces of ZnFe21 films fired at 680°C, 700°C and 720°C. The films fired at 700°C and 720°C had a better flow and bonded to the soda lime silicate glass better than the one that was fired at 680°C. The films fired at 700°C and 720°C were smoother than the one fired at 680°C.

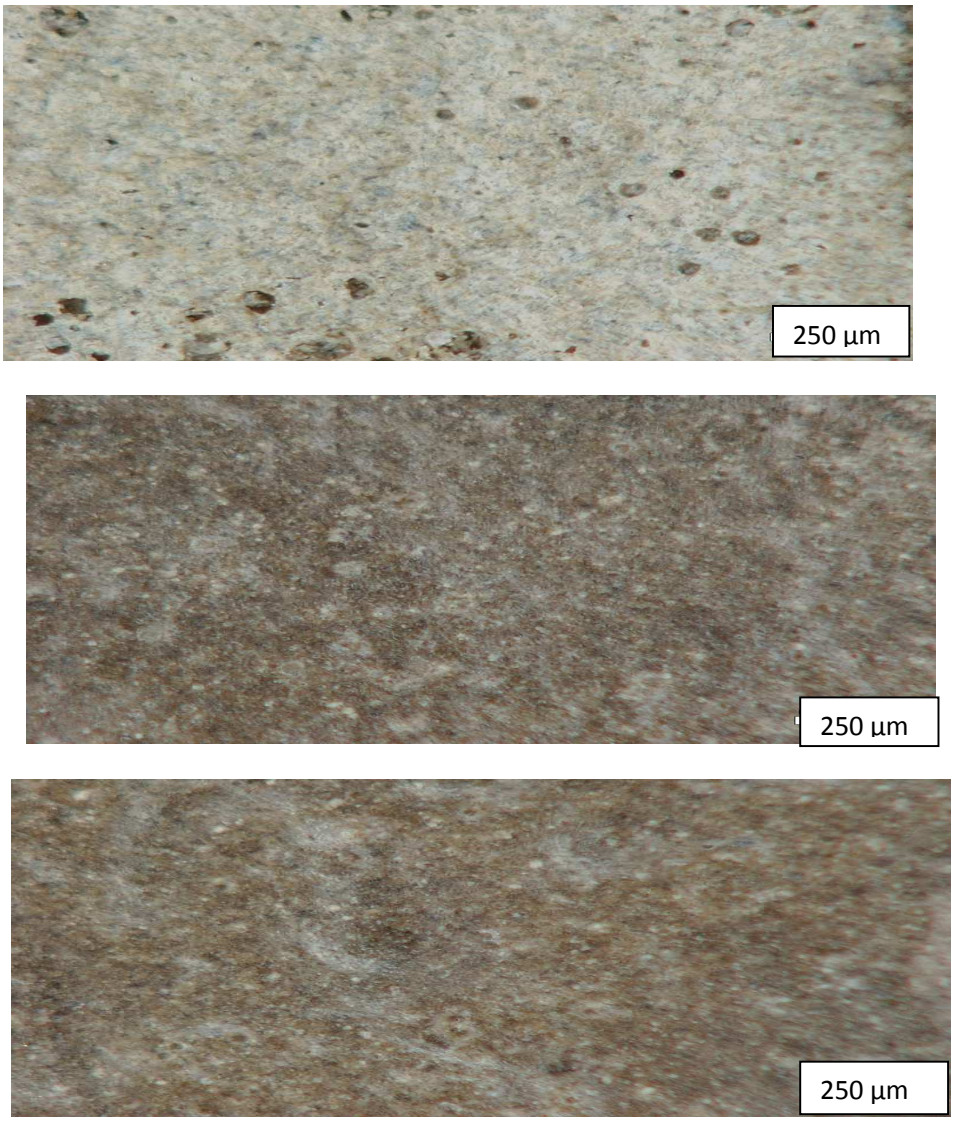

Figure 1.17: Optical micrographs of films of ZnFeP21 fired at 680°C, 700°C and 720°C (top to bottom) for 8 minutes

4. CONCLUSION

The compositional dependence of the properties of $(Na_2O+K_2O)\cdot ZnO\cdot MnO\cdot Fe_2O_3\cdot P_2O_5$ glasses was studied using a design of experiments approach based on a D-optimal design. Twenty compositions were selected that produced nineteen glasses, from which properties of interest for enamel applications were characterized.

It was seen that the effects of increasing alkali (Na_2O+K_2O) content would increase the CTE of the black glasses. Glasses with higher composition of MnO and Fe_2O_3 were more durable and acid-resistant.

The final composition chosen as the optimum composition was designated **ZnFeP21** (in mole % $10ZnO.20MnO.30Fe_2O_3.\ 40P_2O_5$). This glass has a CTE of 10.0×10^{-6}/ °C, a dilatometric softening point of 507°C, and a dissolution rate in HCl(pH~3.4) at 80°C of 7.6×10^{-9} g/cm^2.min . This composition bonded to the soda lime silicate glass well at 680°C, 700°C and 720°C for 8 minutes and had good adherence to the substrate such that the film did not flake off when scratched with our fingernails. The coatings of the glass were grey in color.

PART 2

EFFECT OF MANGANESE OXIDE ON THE PROPERTIES OF ZINC PHOSPHATE GLASSES

1. INTRODUCTION

1.1 INTRODUCTION FOR ZINC MANGANESE PHOSPHATE GLASSES

Phosphate glasses are technologically important materials due to their attractive optical properties, e.g., low dispersion, high ultraviolet transparency, photoluminescence, laser, and amplifier effects [12-16]. Such properties depend strongly on the nature of metal oxides which modify the phosphate structure and on the ratio of metal oxide content to P_2O_5 [17].

Manganese phosphate glasses are of interest for their optical applications [18]. Zinc manganese phosphate glasses (ZnO-MnO-P_2O_5) of different compositions have been synthesized and their optical band gaps have been measured as have photoconduction measurements in the spectral energy range 1.5-6.2 eV [19]. Mn containing glasses showed that Mn ions are present in the +2 or +3 oxidation states [20-26]. Since glasses have the feature of compositional diversity, photoluminescence properties in Mn^{2+} - doped phosphate glasses have been widely studied [27-31].

2. EXPERIMENTAL PROCEDURE

2.1 GLASS FORMATION

Glasses were prepared using reagent grade raw materials including ZnO, MnO and $NH_4H_2PO_4$ for the $ZnO.MnO.P_2O_5$ system and ZnO, Mn_2O_3 and $NH_4H_2PO_4$ for the $ZnO.Mn_2O_3.P_2O_5$ system. The Appendix provides information about the raw material sources. The batch size of all the glasses was 100 grams. The batch powders were ground in a mortar and pestle for five minutes to ensure good mixing, and then added to an aluminosilicate (fireclay) crucible. Batches were pre-reacted at 800°C for 30 minutes to remove ammonia. The crucible with the pre-reacted batch was then transferred to another furnace for melting in air for 2 hours at 1250°C. The crucibles were taken out of the furnace once after 30 minutes and the melts were stirred with a silica rod to help remove bubbles and to improve melt homogeneity. A portion of each melt was cast in molds ($2.5\times1\times0.5$ cm^3) for dilatometry experiments. The remainder of each melt was cast into a mold which had a volume of $1\times1\times1$ cm^3. Glasses were annealed for six hours at 350°C. The glass compositions that were melted are listed in Table I.

Every composition listed in Table I formed a crystal-free glass upon quenching. The glasses were transparent with some bubbles. The glasses varied in color, depending on the concentrations of MnO and Mn_2O_3. The transparency of the glasses decreased with the increase of MnO and Mn_2O_3 with their color ranging from light to dark purple. Other glasses with MnO content of 50 mole % and Mn_2O_3 content of 30, 40 and 50 mole % did not form glasses. They appeared to be crystallized when melts were quenched.

Table I: Glass Compositions (mole %)

ID	P_2O_5	ZnO	MnO
MnZnP1	50	50	0
MnZnP2	50	40	10
MnZnP3	50	30	20
MnZnP4	50	20	30
MnZnP5	50	10	40
ID	**P_2O_5**	**ZnO**	**Mn_2O_3**
Mn2ZnP2	50	40	10
Mn2ZnP3	50	30	20

2.2 DILATOMETRY

Dilatometry was used to measure the glass transition temperature (T_g) and the coefficient of thermal expansion (CTE) for each sample. The samples for the dilatometer were approximately 25 mm in length. These bars were cut with an Isomet low-speed diamond saw and the ends were polished with 600 grit silicon carbide paper. Vernier calipers were used to determine whether the ends were parallel and to measure the sample lengths. An Orton Automatic Recording Dilatometer (Model 1600) was used for these measurements. All measurements were done in air. The sample was heated at a rate of 10°C per minute to about 500°C. The coefficient of thermal expansion (CTE) was calculated over the range of 250 – 350°C. This range was chosen to be below the glass transition temperature (T_g). The CTE was calculated using the slope of the percent linear change (PLC) vs. Temperature curve:

$$CTE = \frac{(PLC_{350} - PLC_{250})/100}{(350-250)^{\circ}C} \quad (1)$$

The glass transition temperature was determined using the intersections of the two extensions of the length change vs. temperature results, above and below T_g. The dilatometric softening temperature (T_d) was taken as the temperature of maximum expansion for each sample, prior to softening.

2.3 CORROSION TESTS

One annealed glass cube (1×1×1 cm^3) from each melt was polished using the 600 and 800 grit silicon carbide paper, and then carefully cleaned using acetone with fresh Kimwipes. Each sample was then immersed in deionized (DI) water with an initial pH of 7.92, contained in Nalgene bottles and maintained at 80°C. The samples were suspended using nylon thread. The glass surface area-to-solution volume ratio was fixed at 0.06 cm^{-1}. The initial weights of the samples were recorded, and the sample weights and the pH of the corresponding solution were recorded after 1 hour, 2 hours, 4 hours and 7 hours on test. The samples were dried for 12 hours at room temperature before recording the weight loss. The pH for all the solutions was recorded after 7 hours of corrosion tests. The dissolution rate (DR) was calculated using the relation,

$$DR = \frac{\Delta W}{SA \times t} \quad (2)$$

where ΔW is the change in weight of the sample after time t, SA is the surface area of the sample, and t is the time in minutes.

2.4 UV-VIS SPECTROSCOPY

The samples that were cast into the 1×1×1 cm^3 were cut using a Isomet low speed diamond saw. The glass samples were polished to a 1200 grit finish on both sides, using SiC paper and water as lubricant. Sample thickness varied around 1 to 1.5 mm. The samples were then polished with 1μm Monocrystalline Diamond Suspension for the absorption experiments. Optical absorption spectra were collected with a Varian Cary 5 UV-VIS spectrophotometer operated in 175-3300 nm range. All these optical spectroscopy were performed at room temperature.

3. RESULTS AND DISCUSSION

3.1 THERMAL PROPERTIES

Table II summarizes the thermal properties for the glasses and the dilatometric curves are in Figure 2.1.

Table II: Summary of Thermal Properties from Dilatometric Measurements

ID		Tg(° C)	Td (° C)	CTE($\times 10^{-6}$/ ° C)
MnZnP1	0MnO	366	412	9.7
MnZnP2	10MnO	383	421	9.2
MnZnP3	20MnO	397	431	10.6
MnZnP4	30MnO	419	449	10.7
MnZnP5	40MnO	451	468	10.9
Mn2ZnP2	$10Mn_2O_3$	399	431	9.9
Mn2ZnP3	$20Mn_2O_3$	426	448	11.1

It can be seen from the above data that replacing ZnO with either MnO or Mn_2O_3 increases the T_g, T_d and the CTE of the glass. These trends are plotted in Figure 2.2.

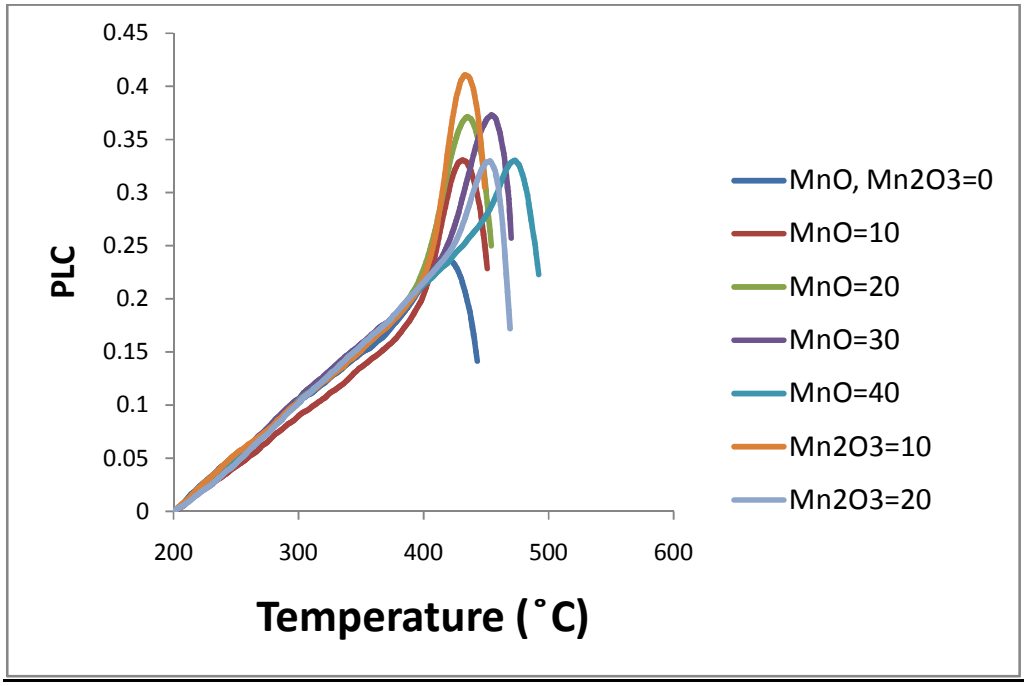

Figure 2.1: Dilatometric curves for the glasses

The glass transition temperature for the 50 $ZnO.50P_2O_5$ glass is lower than what was reported by Ouchetto et al. [32] and Takebe [33]. Those earlier studies both had characterized the glass transition temperature using the DTA (Differential Thermal Analysis) to report the value of T_g between 445-450°C. In addition, Takebe had reported the CTE of his 50 $ZnO.50P_2O_5$ to be 7.1×10^{-6}/ °C.

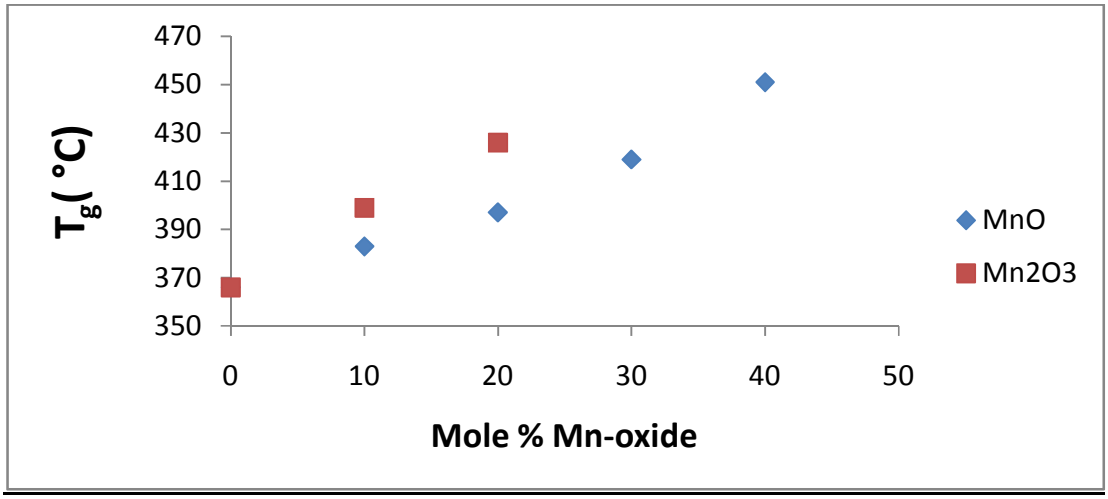

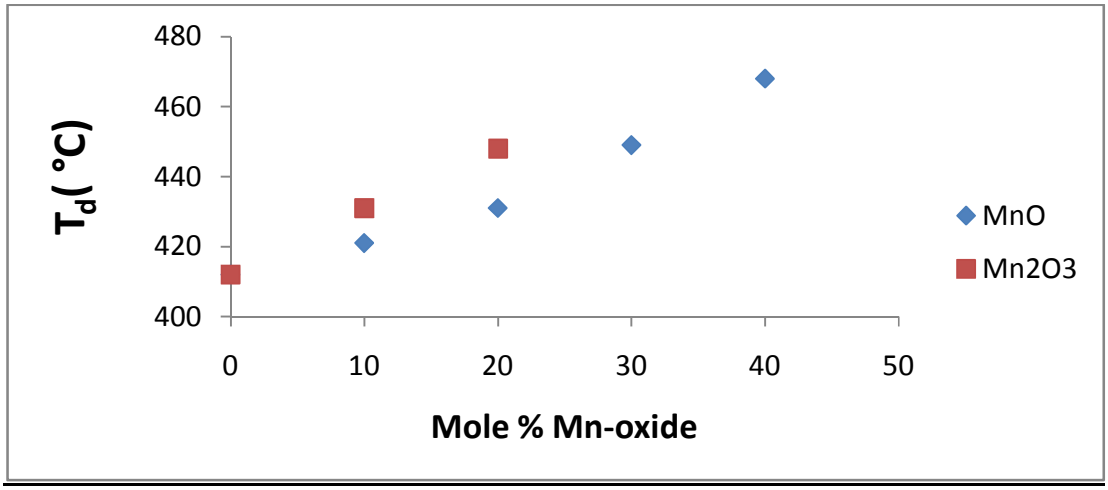

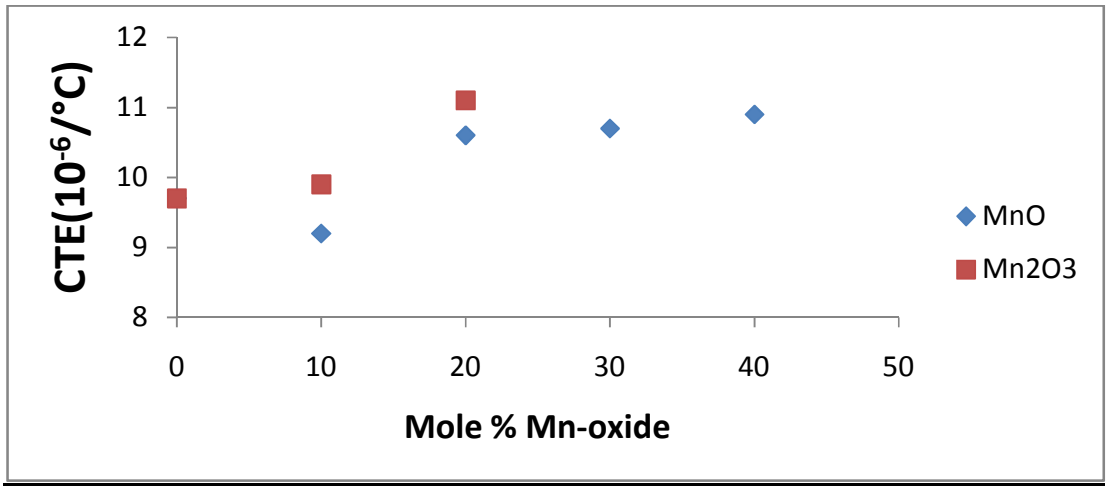

Figure 2.2: Effect of MnO and Mn_2O_3 on the thermal properties

3.2 CORROSION STUDIES

Figures 2.3 and 2.4 show the weight losses for the different glasses at 80°C. It can be seen that the replacement of ZnO by MnO or Mn_2O_3 decreases the weight loss rate. Table III summarizes the total weight losses after different times at 80°C, and the pH of the solution at the conclusion of each experiment. Sample ZnMnP1 fractured after 4 hours in 80°C.

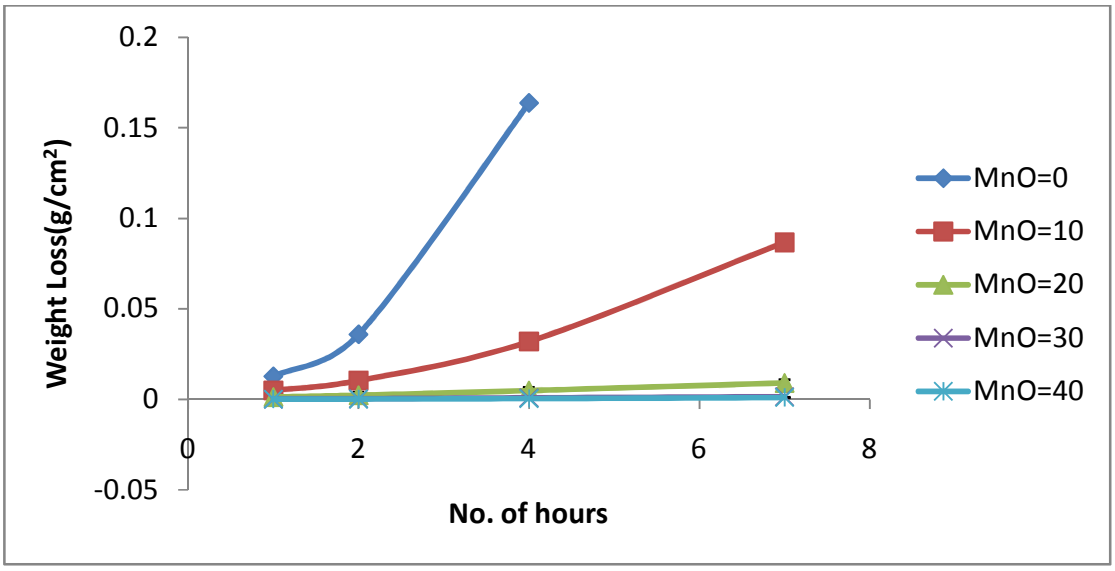

Figure 2.3: Impact of MnO on the weight loss of glasses in DI water at 80°C

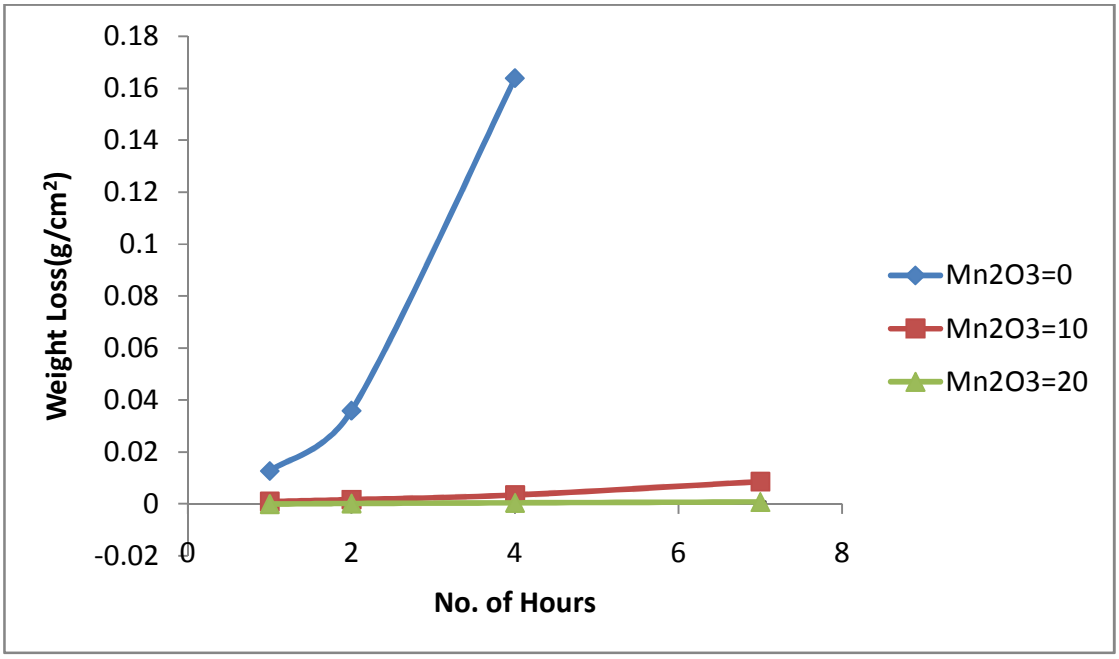

Figure 2.4: Impact of Mn_2O_3 on the weight loss of glasses in DI water at 80°C

Table III: Dissolution rates for glasses in DI water (pH = 7.92) at 80°C

ID	Dissolution Rate (g/ cm^2.min)	Sol'n pH at 7 hours
ZnMnP1	7×10^{-4}	3.0
ZnMnP2	2×10^{-4}	4.0
ZnMnP3	2×10^{-5}	4.9
ZnMnP4	4×10^{-6}	6.1
ZnMnP5	2×10^{-6}	6.0
ZnMn2P2	2×10^{-5}	4.7
ZnMn2P3	2×10^{-6}	5.8

The glasses having the greater content of ZnO dissolve faster than the ones having more of MnO or Mn_2O_3. As a result, the pH of the solutions after 7 hours was lowest for the glasses having the greatest ZnO content and greatest for glasses having the least ZnO content (Figure 2.5). This is because the greater the ZnO content the faster the glasses dissolve in the solution, making the pH more acidic. Previous studies have shown that with greater dissolution of Zn-phosphate glasses the pH also decreases [34]. When phosphate glasses dissolve the solution becomes more acidic because of the formation of phosphoric acid with the release of phosphate ions from the glass into solution.

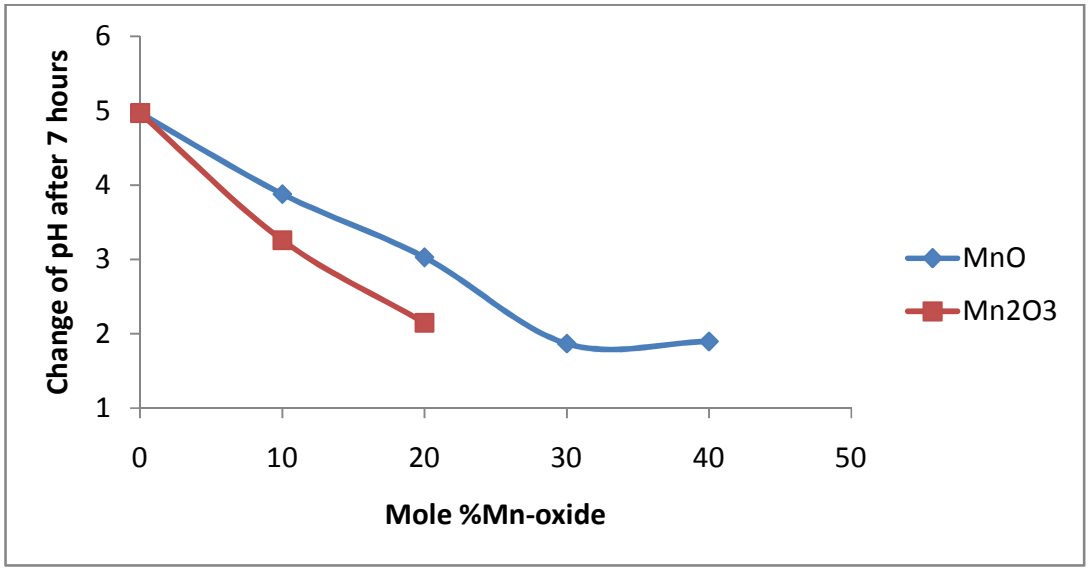

Figure 2.5: Change of pH of the solution with MnO and Mn_2O_3 content

3.3 OPTICAL CHARACTERIZATION

Figures 2.6 and 2.7 shows the UV/VIS spectra collected for the MnO and Mn_2O_3 containing glasses respectively. The narrow peaks at 350 nm and 410 nm are due to Mn^{2+}[18]. The broad peaks at 520 nm are due to Mn^{3+} which is close to the reported Mn^{3+} peak of 530 nm for Sr-Mn metaphosphate glasses [17]. It can be seen in figures 2.8 and 2.9 that the Mn^{3+} has a greater extinction coefficient (ε) than Mn^{2+}. The Beer Lambert law was used to calculate the ε,

$$\frac{A}{d} = c.\varepsilon \qquad (3)$$

where A/d is the absorbance per unit length, C is the concentration in gram per cubic centimeter (g/cc) and ε is the molar extinction coefficient in cc/ g mm. Higher molar absorptivity indicates higher absorption. The glasses with Mn^{3+} had a molar extinction

coefficient of 6.3 cc/ g mm while glasses whereas Mn^{2+} had a molar extinction coefficient of 4.5 cc/ g mm.

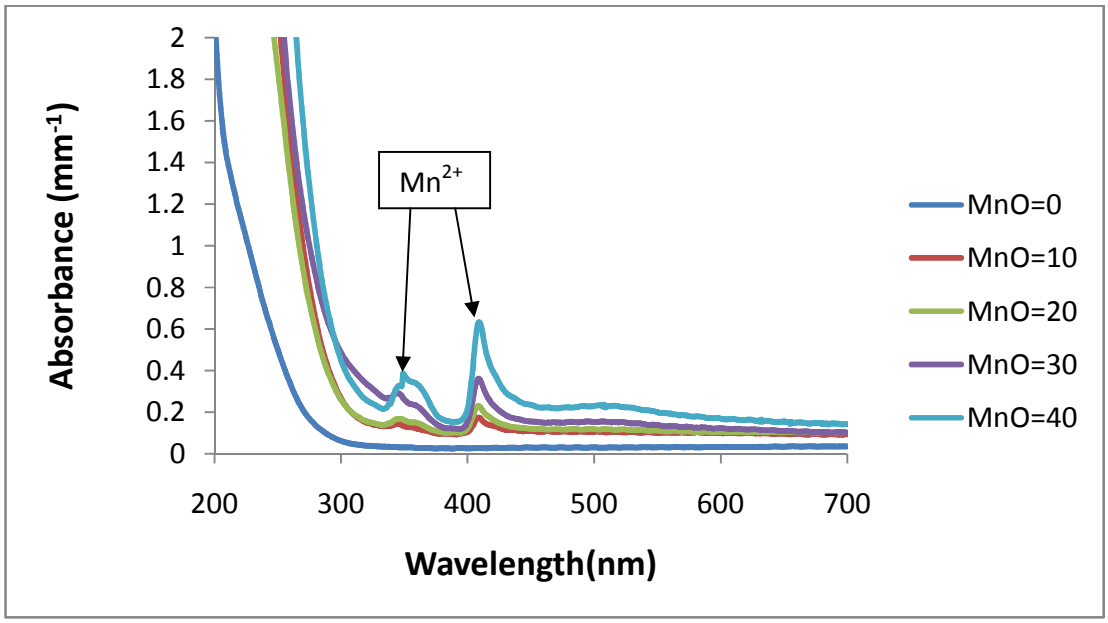

Figure 2.6: Effect of MnO on the UV-VIS spectra of the glasses

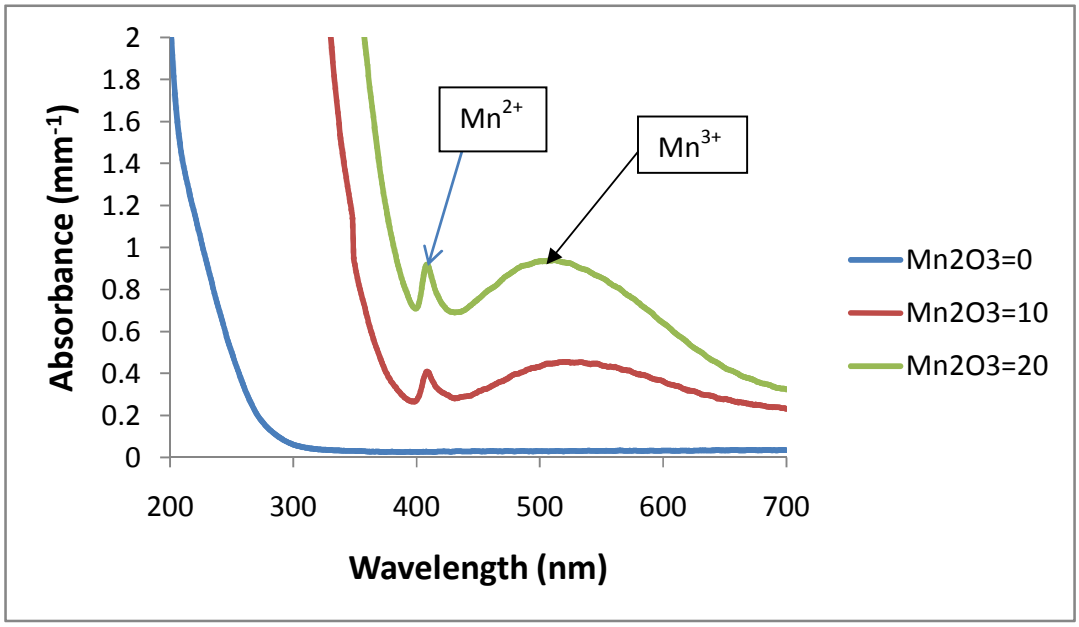

Figure 2.7: Effect of Mn_2O_3 on the UV-VIS spectra of the glasses

While the Mn-free glass shows no absorption in the visible range, introduction of MnO leads to development of absorption bands at 410 nm and 530 nm which result from d-d electronic transitions of Mn^{2+} (d^5) and Mn^{3+}(d^4) ions respectively[20-26,35-39]. The glass absorption edge shifts to the visible range with increasing MnO content as a result of very intense charge-transfer excitations from oxygen to Mn^{2+} and Mn^{3+} ions and because of the intervalence charge-transfer excitations between Mn^{2+} and Mn^{3+} ions at high manganese contents [20,21,24].

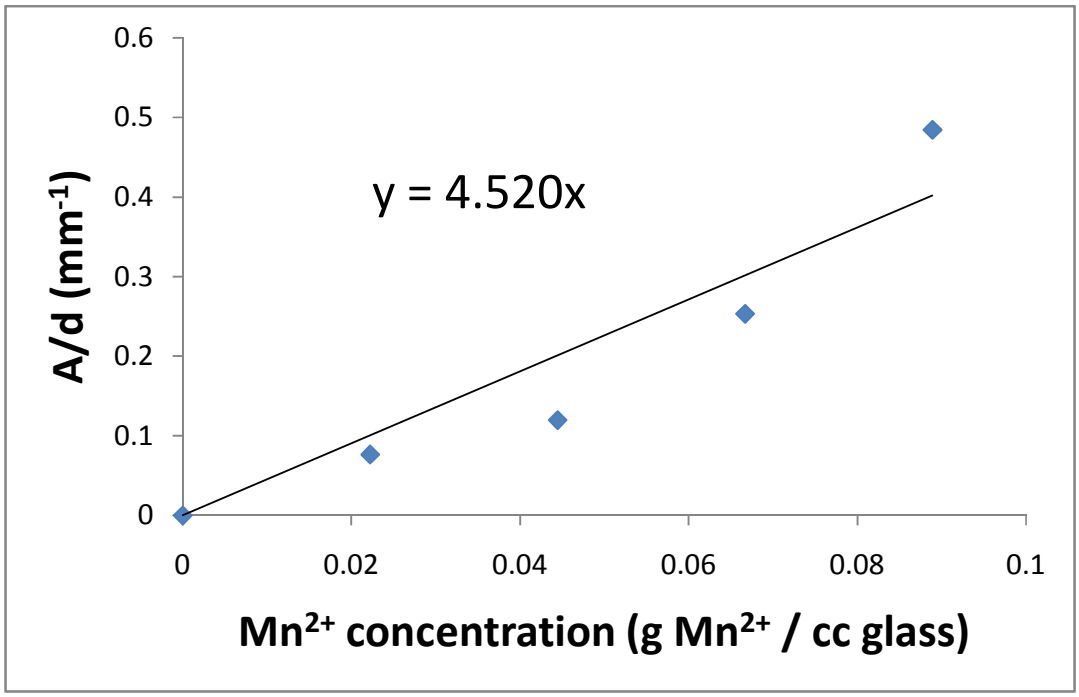

Figure 2.8: A/d change at 410 nm. with Mn^{2+} concentration

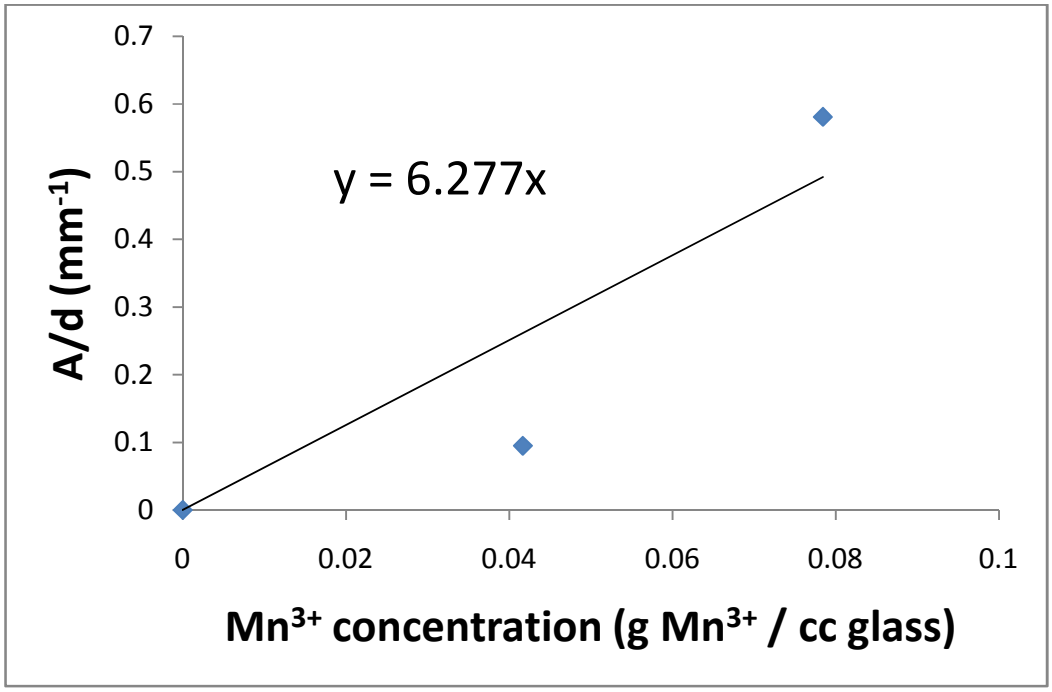

Figure 2.9: A/d change at 520 nm. with Mn^{3+} concentration

4. CONCLUSION

Glasses of the system (50-x)ZnO.xMnO.50P_2O_5 were made with x=0, 10, 20, 30, 40, 50. All the compositions showed glass forming capability except for 50MnO.50 P_2O_5. The glasses formed were transparent and had small bubbles in them. An increase of MnO content within this system led to an increase in the chemical stability of these glasses. The increase of MnO content also had significant impact on its thermal properties by increasing the CTE, T_g and T_d. The UV-VIS spectra for these glasses show a higher absorption for the glasses with the higher MnO content. This can be attributed to the higher concentration of Mn^{2+} of these glasses.

Glasses of the system (50-x)ZnO.xMn_2O_3.50P_2O_5 were made but only composition of x=0,10,20 were possible. These glasses turned out to be darker than the ones with MnO. With the increase of Mn_2O_3 CTE, T_d and T_g increased. The durability of these glasses also increased with the increase of Mn_2O_3. The addition of Mn_2O_3 increased the absorption of the glasses due to the higher concentration of Mn^{3+}.

Appendix: Raw materials used to prepare glasses for D-optimal design

$NH_4H_2PO_4$: Alfa Aesar 98%.
Stock # 11598
CAS # 7722-76-1
Lot # F18S044

K_2CO_3: Alfa Aesar 99%.
Stock # A16625
CAS # 584-08-7
Lot # C16S026

Na_2CO_3: Alfa Aesar 85% min.
Stock # 14108
CAS # 5968-11-6
Lot # D04L19

Fe_2O_3: Alfa Aesar 99.5%.
Stock # 12375
CAS # 1309-37-1
Lot # C20S036

MnO: Aldrich
CAS # 1344-43-0
Batch # 01301HOLO

ZnO: Aldrich
CAS # 1314-13-2
Batch # 06328D1

Mn_2O_3: Aldrich
CAS # 1317-34-6
Batch # 13160LUM0

BIBLIOGRAPHY

[1] TJ Brown, GE Sakoske, US Patent Number US 2006/0260734 A1, May 18, 2005.

[2] G.E. Sakoske, US Patent Number 005714420, Dec 8, 1995.

[3] S.T. Reis, M. Karabulut, D.E. Day, J. Non-Cryst. Solids 292, 2001, 150.

[4] J.E. Shelby, Introduction to Glass Science and Technology, RSC, Cambridge, 1997.

[5] G. K. Marasinghe, M. Karabulut, C.S. Ray, D.E. Day, M.G. Shumsky, W.B. Yelon, C.H. Booth, P.G. Allen, D.K. Shuh, J. Non-Cryst. Solids 222, 1997, 144.

[6] N.H. Ray, "Inorganic Polymers" Academic Press, New York, 1978.

[7] H.S. Lui, P.Y. Shih, and T.S. Chin, Phys. Chem. Glasses, 37(6), 1996, 227.

[8] T. Jermoumi, M. Hafid, N. Niegisch, M. Menning, A. Sabir, N. Toreis, Materials Research Bulletin 37(1), 2002, 49.

[9] Kristin A. Miller, "Iron Phosphate Glasses for Black Enamels on Window Glass," MS Thesis, December 2003.

[10] Loretta Francis, "Low-temperature phosphate glass for enameling applications," MS Thesis May 2006.

[11] Larry Kovacic, Stephen V. Crowder, Richard K. Brow, Denise N. Bencoe, Conference:96. Annual meeting of the American Ceramic Society(ACerS)), 25-28 Apr 1994, Ceram. Trans. 70, 177-187, 11/1995.

[12] Weber, M.J. *J. Non-Cryst. Solids* 1990, 123, 208-222.

[13] Vogel, W. Glass Chemistry, 2nd ed.; Springer-Verlag: Berlin, 1994.

[14] Ebendorff-Heidepriem, H.; Seeber, W.; Ehrt, D. *J. Non-Cryst. Solids* 1995, 183, 191-200.

[15] Campbell, J. H.; Suratwala, T.I. *J. Non-Cryst. Solids* 2000, 263&264, 318-341.

[16] (a) Ehrt, D.; Ebeling, P.; Natura, U. *J. Non-Cryst. Solids* 2000, 263&264, 240-250. (b) Ehrt, D.C.R. *Chimie* 2002, 5, 679-692.

[17] Ioannis Konidakis, Christos-Platon E. Varsamis, Efstratios I. Kamitsos, Doris Moncke and Doris Ehrt *J.Phys. Chem.* C 2010, 114, 9125-9138.

[18] Mizuyo Kawano, Hiromichi Takebe, Makoto Kuwabara, Optical Materials 32 (2009) 277–280.

[19] S.A. Siddiqi, M.A. Ghauri and M.J.S. Baig, "The Band Gap Estimation of Zinc Manganese Phosphate Glasses," Modern Physics Letters B Pakistan, No. 12(2008) 1265-1272.

[20] Wong, J.; Angell, C. A. Glass structure by spectroscopy; M. Dekker Inc.: New York, 1976.

[21] Bates, T. Modern aspects of the vitreous state; Mackenzie, J. D., Ed.; Butterworth Inc.: Washington DC, USA, 1962.

[**22]** Ferguson, J. Prog. Inorg. Chem. 1970, 12, 158

[**23]** Carlin, R. L. J. Chem. Educ. 1963, 40, 135– 142

[**24]** Duffy, J. A. Bonding energy levels & bands in inorganic solids; Longman Group UK Limited, 1990.

[**25]** Duffy, J. A.; Ingram, M. D.; Fong, S. Phys. Chem. Chem. Phys. 2000, 2, 1829–1833

[**26]** Fong, S. Ph.D. thesis,University of Aberdeen, Aberdeen, UK, 2002.

[27] I.E.C. Machado, L. Prado, L. Gomes, J.M. Prison and J.R. Martinelli, *J. Non-Cryst. Solids* **348** (2004)

[28] M.C. Flores J., U. Caldino G., J. Hernandez A., E. Camarillo G., E. Cabrera B., H.D. Castillo, A. Speghini, M. Bettinelli, H. Murrieta S., Phys. Stat. Sol. 4 (2007) 922.

[29] D. Ehrt, *J. Non-Cryst. Solids* (2004).

[30] K. Bingham and S. Parke, *Phys. Chem. Glasses* **6** (1965)

[31] S. Parke, A.I. Watson and R.S. Webb, *J. Phys. D: Appl. Phys.* (1970).

[32] M. Ouchetto, B. Elouadi and S. Parke, Phys. Chem. Glasses 32 (1) (1991) 22.

[33] T. Kubo, J. Cha, H. Takebe, M. Kuwabara, Phys. Chem. Glasses: Eur. J. Glass Sci. Technol. B, February 2009, 50(1), 15-18.

[34] H. Takebe, Y. Baba, M. Kuwabara, Journal of Non-Crystalline Solids 352(2006) 3088-3094.

[**35]** Heidt, L. J. Koster, G. F.,Johnson, A. M. J. Am. Chem. Soc. 1958, 80, 6471– 6477

[**36]** Nelson, C.; White, W. B. Geochim. Cosmochim. Acta 1980, 44, 887– 893

[**37]**Kohler, P., Massa, W., Reinen, D. Z. Anorg. Allg. Chem. 1978, 446, 131– 158

[**38]** Kawano, J. M.; Takebe, H.; Kuwabara, M. Opt. Mater. 2009, 32, 227– 280

[**39]** Machado, I. E. C. Prado, L. Gomes, L. Prison, J. M. Martinelli, J. R. J. Non-Cryst. Solids 2004, 348, 113– 117

VITA

Sagnik Saha was born on February 28, 1985 to Bimal and Bratati Saha in Kolkata, India. He completed his schooling in Don Bosco Park Circus, India. After completing his schooling in April 2003 he moved to USA and started his Bachelors at Coe College, Iowa where he got a BA degree with a major in Physics and Math. Sagnik was a part of the “Steve Feller Research Group” for several years while he was pursuing his Bachelors degree. He then began his Masters in August 2007 at the Missouri University of Science and Technology where he worked as a Graduate Research Assistant under the direct supervision of Dr. Richard K. Brow. Sagnik also received a Lean-Six Sigma graduate certificate from the Engineering Management Dept. and graduated with a Masters in Materials Science and Engineering in December 2010.